European Journal of Medicinal Chemistry xxx (2017) 1–19

Contents lists available at ScienceDirect

European Journal of Medicinal Chemistry

journal homepage: http://www.elsevier.com/locate/ejmech

Research paper

Design, synthesis and biological evaluation of novel benzimidazole amidines as potent multi-target inhibitors for the treatment of non-small cell lung cancer

Andrea Bistrović [a], Luka Krstulović [b], Anja Harej [c], Petra Grbčić [c], Mirela Sedić [c, **], Sanja Koštrun [d], Sandra Kraljević Pavelić [c], Miroslav Bajić [b], Silvana Raić-Malić [a, *]

[a] Department of Organic Chemistry, Faculty of Chemical Engineering and Technology, University of Zagreb, Marulićev Trg 20, HR-10000 Zagreb, Croatia
[b] Department of Chemistry and Biochemistry, Faculty of Veterinary Medicine, University of Zagreb, Heinzelova 55, HR-10000 Zagreb, Croatia
[c] Department of Biotechnology, Center for High-Throughput Technologies, University of Rijeka, Ulica Radmile Matejčić 2, HR-51000 Rijeka, Croatia
[d] Chemistry Department, Fidelta Ltd., Prilaz Baruna Filipovića 29, HR-10000 Zagreb, Croatia

ARTICLE INFO

Article history:
Received 17 May 2017
Received in revised form
18 October 2017
Accepted 20 October 2017
Available online xxx

Keywords:
Benzimidazole
1,2,3-triazole
Kinase
p38 MAPK
Multitarget
Non-small cell lung cancer (A549)

ABSTRACT

A series of novel amidino 2-substituted benzimidazoles linked to 1,4-disubstituted 1,2,3-triazoles were synthesized by implementation of microwave and ultrasound irradiation in click reaction and subsequent condensation of thus obtained 4-(1,2,3-triazol-1-yl)benzaldehyde with *o*-phenylenediamines. *In vitro* antiproliferative screening of compounds performed on human cancer cell lines revealed that *p*-chlorophenyl-substituted 1,2,3-triazolyl *N*-isopropylamidine **10c** and benzyl-substituted 1,2,3-triazolyl imidazoline **11f** benzimidazoles had selective and potent cytostatic activities in the low nM range against non-small cell lung cancer cell line A549, which could be attributed to induction of apoptosis and primary necrosis. Additional Western blot analyses showed different mechanisms of cytostatic activity between compounds **10c** and **11f** that could be associated with the nature of aromatic substituent at 1-(1,2,3-triazolyl) and amidino moiety at C-5 position of benzimidazole ring. Specifically, compound **11f** abrogated the activity of several protein kinases including TGM2, CDK9, SK1 and p38 MAPK, whereas compound **10c** did not have profound effect on the activities of CDK9 and TGM2, but instead showed moderate downregulation of SK1 activity concomitant with a significant reduction in p38 MAPK. Further *in silico* structural analysis demonstrated that compound **11f** bound slightly better to the ATP binding site of p38 MAPK compared to **10c**, which correlated well with observed stronger decrement in the expression level of phospho-p38 MAPK elicited by **11f** in comparison with **10c**.

1. Introduction

Lung cancer is the leading cause of cancer-related mortality worldwide [1,2]. Non-small cell lung cancer (NSCLC), which includes adenocarcinoma, squamous cell carcinoma, and large cell carcinoma, accounts for approximately 85% of all lung cancers, with only 17% predicted 5-year survival rate in all stages, and approximately 2% predicted 5-year survival rate in stage IV [3–5]. Although the treatment of non-small cell lung cancer has evolved over the past decade resulting in a delivery of different therapeutic options, chemotherapy produces only a small improvement in the survival of patients with advanced NSCLC [6]. Thus, novel treatment strategies for combating this disease are urgently needed.

Protein kinases play important roles in diverse molecular mechanisms regulating cell division, growth, and death [7,8]. They are involved in intracellular signaling processes by catalyzing the transfer of the γ-phosphate of ATP to downstream protein substrates [9]. In addition to their key roles in cell physiology, about half of protein kinases are linked to pathological states including cancer [10,11]. This fact makes kinases attractive targets for therapeutic intervention. The identification of small molecules targeting protein kinases has become one of the milestones in the development of anticancer drugs [12].

Over the past years, in the search for novel chemotherapeutic agents, a new generation of versatile benzimidazole-based

* Corresponding author.
** Corresponding author.
E-mail address: sraic@fkit.hr (S. Raić-Malić).

https://doi.org/10.1016/j.ejmech.2017.10.061
0223-5234/

derivatives with potent antitumor activity has been developed. Besides their function as DNA binding agents [13,14], benzimidazoles have been identified as potent inhibitors of protein kinases [12]. Majority of the clinically approved kinase inhibitors include bicyclic nitrogen hetrocycles, such as purine or purine isosters [15]. Besides, benzimidazole scaffold is recognized as a common moitey that interacts with kinases by multiple binding modes [16–18]. The substitution at 1, 2, 5 and/or 6 positions of the benzimidazole moiety was crucial for their activities towards several kinases, such as mitogen activated protein kinase (MAPK), aurora kinase, polo like kinase and Tie kinase [12]. Furthermore, some benzimidazole-based derivatives with anticancer and proapoptotic activity were developed as selective inhibitors of protein kinase CK2 (casein kinase II) [19–21]. Compounds containing fluoro-substituted benzimidazole core were in clinical trials as cyclin-dependent kinase 9 (CDK9) inhibitors for treatment of cancer [22]. Over the years, protein kinase inhibitors have shown therapeutic limitations mainly resulting from drug resistance due to mutations or the activation of alternative pathways, poor selectivity, and off-target effects [23]. For these reasons, in recent years, multitarget approaches directed towards inhibition of kinases and targets of different families have received increasing attention [24–26]. Thus, some benzimidazole derivatives have been also developed as multi-target inhibitors [27–31]. Moreover, dovitinib (TKI258/CHIR258) is a multi-kinase inhibitor in phase III clinical trials for the treatment of several cancers [32].

On the other hand, 1,2,3-triazole core was also found as a binding motif in potent inhibitors of different protein kinases [33–40]. 1,2,3-Triazole heterocycles have been recognized as good amide bioisosteres [41]. It has been found recently that 1,2,3-triazolyl derivative inhibits the activity of transglutaminase 2 (TGM2) by inducing its conformational change to closed form [42]. Moreover, cinnamoyl triazole derivatives acting as reversible inhibitors showed to compete with acyl donor TGM2 substrates [43].

In our previous study of *N*-heterocyclic compounds as anticancer agents, we found that combination of benzimidazole and 1,2,3-triazole moieties exerted potent and selective cytostatic effect against hepatocellular carcinoma cells in nM range [44]. Among diverse C-4 substituents at 1,2,3-triazole ring, the *p*-substituted phenyl led to increased antiproliferative activity compared to aliphatic branched or unbranched C-4 side chains. Moreover, halophenyl-substituted 1,2,3-triazolyl in bioactive hybrids contributed to strong cytostatic activity in hepatocellular carcinoma cells associated with Wee-1 kinase inhibition [33]. In addition, amongst the aromatic diamidines, bis(amidinophenyl)-derived heterocycles showed strong antiproliferative activity against cervical carcinoma cells [45]. In view of the biological importance of benzimidazoles and 1,2,3-triazoles, and as a part of ongoing research focused on the development of new anticancer agents, we aimed to design and synthesize multi-target hybrid chemical entities by the fusion of both pharmacophoric ring systems in a single molecular framework that would result in pronounced antiproliferative activities and reduced chemoresistance by inhibiting multiple molecular targets (Fig. 1).

In this context, amidino 2-substituted benzimidazoles were linked *via* phenoxymethylene, ethylene spacer or directly to the 1,2,3-triazole ring with a diverse *p*-substituted phenyl or benzyl subunit at *N*-1, thus containing distributed highly hydrophilic and hydrophobic part of the structure. Antiproliferative effects of benzimidazoles with 1,4-disubstituted 1,2,3-triazole on selected human tumor cell lines were evaluated, and the structure-activity relationship (SAR) was discussed. The compounds **10c** and **11f** with potent and selective antiproliferative activity on non-small cell lung cancer (A549) were selected for more detailed investigation of their mechanism of action. Specifically, induction of

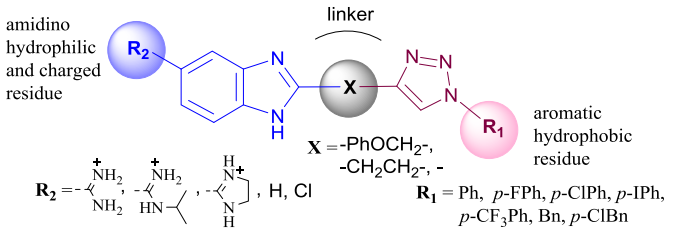

9a–9f, **10a–10g**, **11a–11g**, **12c**, **13c**, **19a**, **19b** and **20a**

Fig. 1. Design and synthesis of amidine derivatives of benzimidazole-1,2,3-triazole conjugates containing non-substituted and halogen-substituted aromatic moiety.

apoptosis and validation of potential protein targets for **10c** and **11f** by Western blot were carried out. Since p38 mitogen-activated protein kinase (MAPK) was identified as one of the possible protein targets for both compounds, structural analysis of binding interactions within the ATP-binding pocket was performed by molecular docking.

2. Results and discussion

2.1. Chemistry

The synthesis of novel 1,2,3-triazolyl linked 2-aryl benzimidazole derivatives (**9a–9f**, **10a–10g**, **11a–11g**, **12c** and **13c**) was carried out as shown in Scheme 1. 4-*O*-Propargylated benzaldehyde (**2**) was synthesized from the 4-hydroxy benzaldehyde with propargyl bromide, which was then used as a dipolarophile in the regioselective Cu(I) catalyzed cycloaddition with unsubstituted, *para*-halogen- and *para*-trifluoromethyl-substituted phenyl azides

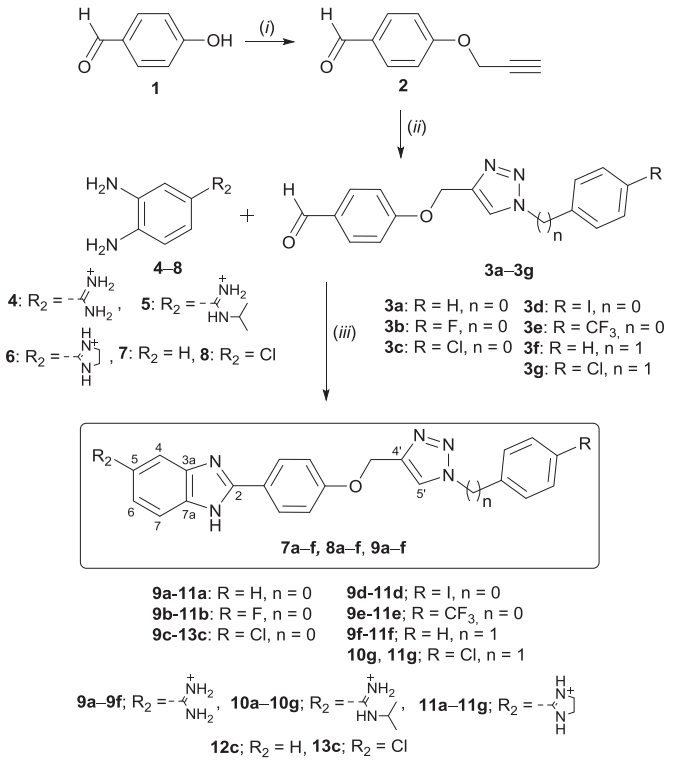

Scheme 1. *Reagents and reaction conditions*: (*i*): propargyl bromide, K_2CO_3, EtOH, reflux, 24 h; (*ii*): azide, $CuSO_4$, Cu(0), DMF, *t*-BuOH: H_2O = 1: 1, 80 °C, 1.5 h, MW/US; (*iii*): a) 1,2-phenylenediamine (**4–8**), $NaHSO_3$, EtOH, reflux, 6 h; b) HCl/MeOH, rt, 4 h.

Please cite this article in press as: A. Bistrović, et al., Design, synthesis and biological evaluation of novel benzimidazole amidines as potent multi-target inhibitors for the treatment of non-small cell lung cancer, European Journal of Medicinal Chemistry (2017), https://doi.org/10.1016/j.ejmech.2017.10.061

to afford **3a**–**3g**. In the recent years, microwave and sonochemical methods have proven to be powerful techniques for facilitating various chemical reactions [46–48]. Therefore, greener methods using ultrasound and microwave irradiation were applied in click chemistry of 1,2,3-triazoles **3a**–**3g** in the presence of Cu(I) catalyst, which was generated *in situ* from Cu(II) sulfate and metallic copper. It was indicated that acoustic cavitation effect of ultrasound-assisted reaction was more beneficial for the heterogeneous copper-catalyzed click reactions affording 1,2,3-triazole products **3a**–**3g** in higher yields (62–99%) than those performed under microwave irradiation (30–71%). Condensation of various *o*-phenylenediamines (**4**–**8**) with 4-(1,2,3-triazol-1-yl)benzaldehyde derivatives (**3a**–**3g**) using $NaHSO_3$ [49], as an oxidative reagent, afforded the target 5-amidino-substituted benzimidazoles **9a**–**9f**, **10a**–**10g** and **11a**–**11g**, non-substituted benzimidazole **12c** and 5-chloro-substituted benzimidazole **13c**. Amidino-substituted *o*-phenylenediamines (**4**–**6**) were prepared by the Pinner method as previously reported in the literature [50].

With the aim to assess the influence of the phenoxymethylene linker between the benzimidazole and 1,2,3-triazole moieties on the antiproliferative activities, the 1,2,3-triazole ring was introduced directly (**19a** and **19b**) or *via* an ethylene linker (**20a**) to the benzimidazole ring, as displayed in Scheme 2.

1-(*p*-Chlorophenyl)-1,2,3-triazolyl aliphatic alcohols (**15** and **16**) were prepared in excellent yields in ultrasound-assisted reaction of 4-chlorophenylazide and propargyl alcohol or pentynol using $Cu(OAc)_2$. 1-(*p*-Chlorophenyl)-1,2,3-triazolyl aldehydes (**17** and **18**), as intermediates for the synthesis of 5-amidino benzimidazoles (**19a**, **19b** and **20a**), were subsequently obtained by the Swern oxidation [51].

2.2. Biological profiling

2.2.1. In vitro antiproliferative activity

The results of antiproliferative evaluations of **9a**–**9f**, **10a**–**10g** and **11a**–**11g**, **12c**, **13c**, **19a**, **19b** and **20a** performed on human tumor cell lines including non-small cell lung cancer (A549), ductal pancreatic adenocarcinoma (CFPAC-1), cervical carcinoma (HeLa) and metastatic colorectal adenocarcinoma (SW620) as well as on normal human lung fibroblasts (WI38) are presented in Table 1. 5-Fluorouracil was used as the reference drug.

The *p*-chlorophenyl-substituted 1,2,3-triazolyl derivatives of amidine **9c**, *N*-isopropyl amidine **10c** and imidazoline **11c** exhibited remarkable antiproliferative activities with IC_{50} of 0.05 and 0.06 μM in non-small cell lung cancer cells A549. Interestingly, benzyl-substituted 1,2,3-triazolyl analogue of imidazoline **11f** exerted both, strong and selective inhibitory effect (IC_{50} = 0.07 μM) on A549 cells. Besides, 1-(*p*-iodophenyl)-1,2,3-triazolyl *N*-isopropylamidine **10d** showed also marked cytostatic effects on A549 cells albeit with less selectivity. Taking into account the submicromolar and low micromolar (<5 μM) potencies, relationship between the nature of *p*-substituent at phenyl ring and their activities revealed that cytostatic effects decreased in the following order: I > CF_3 > Cl > F. On the contrary to this, unsubstituted phenyl (in **9a**, **10a**, **11a**) and benzyl subunits (in **9f**, **10f**, **11f**) led to reduced or loss of the activity, with only exception of anti-lung cancer activity of imidazoline **11f**. Introduction of methylene linker between *p*-chlorophenyl and 1,2,3-triazole ring in **10g** and **11g** generally reduced their activity relative to their counterparts **10c** and **11c**, respectively. However, this structural modification resulted in an extremely potent activity (IC_{50} = 0.05 μM) of *p*-chlorobenzyl-substituted 1,2,3-triazolyl analog of imidazoline **11g** against colorectal adenocarcinoma (SW620). This compound also showed selectivity in its antiproliferative effect exhibiting >100-fold lower activities on A549, CFPAC-1 and HeLa cells, relative to SW620 cells. *p*-Iodophenyl subunit in **9d**, **10d**, **11d** contributed to enhanced antiproliferative effect on SW620 cells displaying activities in submicromolar range (**9d**, IC_{50} = 0.95 μM; **10d**, IC_{50} = 0.69 μM; **11d**, IC_{50} = 0.37 μM). The type of cationic moiety at the benzimidazole core had also impact on the antiproliferative activities. Thus, considering the submicromolar activities among the amidino-substituted benzimidazole series, imidazolines **11a**–**11f** were the most potent, whereas *N*-isopropylamidines **10a**–**10f** showed the lowest overall activity. Besides the abovementioned highly potent effects of imidazolines **11c** and **11f** on A549 cells, imidazolino fragment was mainly responsible for the inhibitory effect on cervical carcinoma cells HeLa. Thus, imidazolines **11a**–**11g** showed antiproliferative activity against HeLa cells with IC_{50} in the range of 0.22–7.78 μM. In addition, *p*-iodophenyl and *p*-(trifluoromethyl) phenyl analogs **11d** and **11e** of imidazolines exhibited submicromolar activity on pancreatic carcinoma (CFPAC-1). Except for **10b**, all amidines (**9a**–**9f**) and *N*-isopropylamidines (**10a**, **10c**–**10g**) either exhibited reduced potencies or were deprived of any activities. Replacement od phenoxymethylene with ethylene linker or

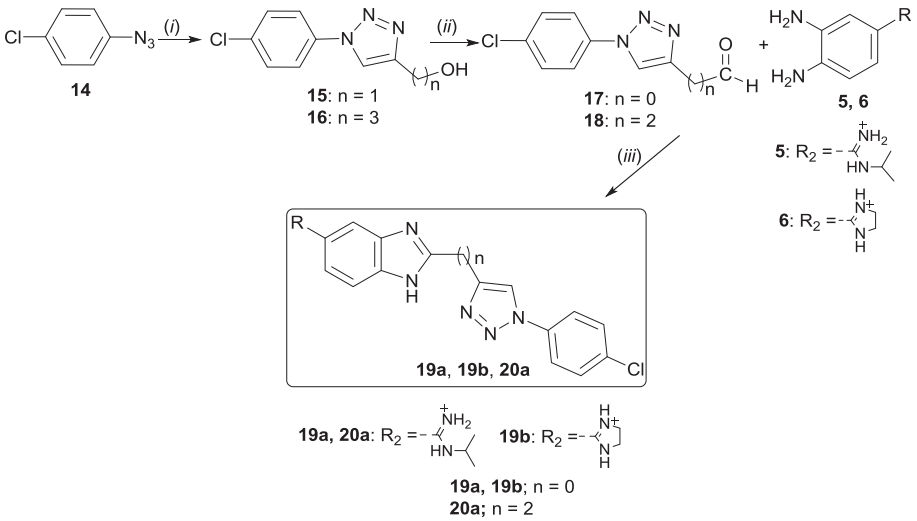

Scheme 2. *Reagents and reaction conditions*: (*i*): propargyl alcohol/4-pentyn-1-ol, $Cu(OAc)_2$, MeOH, 80 °C, US, 1.5 h; (*ii*): $(COCl)_2$, DMSO, Et_3N, CH_2Cl_2, -78 °C to rt 45 min; (*iii*): a) 1,2-phenylenediamine (**5** and **6**), $NaHSO_3$, EtOH, reflux, 6 h; b) HCl/MeOH, rt, 4 h.

Please cite this article in press as: A. Bistrović, et al., Design, synthesis and biological evaluation of novel benzimidazole amidines as potent multi-target inhibitors for the treatment of non-small cell lung cancer, European Journal of Medicinal Chemistry (2017), https://doi.org/10.1016/j.ejmech.2017.10.061

Table 1
In vitro growth inhibitory effects of compounds **9a**–**9f**, **10a**–**10g**, **11a**–**11g**, **12c**, **13c**, **19a**, **19b** and **20a** on human tumor cell lines.

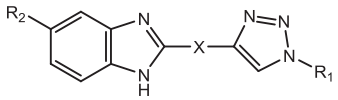

Compd	R_1	X	R_2	IC_{50}[a] (μM)				
				A549	CFPAC-1	HeLa	SW620	WI38
9a		-PhOCH$_2$-		53.31	29.87	18.84	31.51	8.08
9b	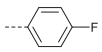	-PhOCH$_2$-		80.97	>100	7.39	37.85	0.70
9c	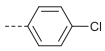	-PhOCH$_2$-		0.05	18.54	0.80	7.57	5.03
9d	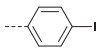	-PhOCH$_2$-		0.45	21.48	6.45	0.95	0.62
9e	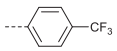	-PhOCH$_2$-		0.84	2.09	0.32	0.36	0.52
9f		-PhOCH$_2$-		9.47	34.44	13.71	30.91	0.89
10a		-PhOCH$_2$-		>100	>100	16.60	62.14	0.99
10b	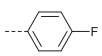	-PhOCH$_2$-		8.37	0.71	0.59	37.85	0.66
10c	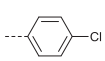	-PhOCH$_2$-		0.05	>100	17.53	48.69	8.04
10d	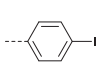	-PhOCH$_2$-		0.08	5.13	0.51	0.69	0.20
10e	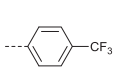	-PhOCH$_2$-		85.76	>100	13.72	50.15	0.32
10f		-PhOCH$_2$-		6.18	>100	8.80	58.61	65.41
10g		-PhOCH$_2$-		4.98	>100	>100	36.48	0.70
11a		-PhOCH$_2$-	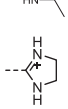	49.69	26.21	7.78	29.63	0.10
11b	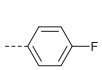	-PhOCH$_2$-	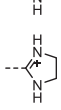	>100	>100	0.98	2.31	0.09
11c	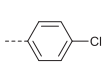	-PhOCH$_2$-	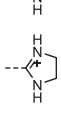	0.06	16.88	0.22	3.65	2.24
11d	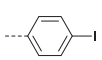	-PhOCH$_2$-	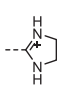	>100	0.86	0.42	0.37	0.22
11e	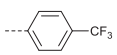	-PhOCH$_2$-	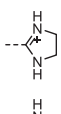	0.59	0.65	2.69	6.35	0.69
11f		-PhOCH$_2$-	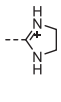	0.07	29.17	6.67	28.05	6.89

Please cite this article in press as: A. Bistrović, et al., Design, synthesis and biological evaluation of novel benzimidazole amidines as potent multi-target inhibitors for the treatment of non-small cell lung cancer, European Journal of Medicinal Chemistry (2017), https://doi.org/10.1016/j.ejmech.2017.10.061

Table 1 (*continued*)

Compd	R_1	X	R_2	IC_{50}[a] (μM)				
				A549	CFPAC-1	HeLa	SW620	WI38
11g	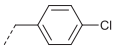	-PhOCH$_2$-		9.34	6.82	5.06	0.05	5.77
12c	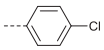	-PhOCH$_2$-	H	7.96	>100	>100	99.26	1.11
13c	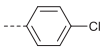	-PhOCH$_2$-	Cl	2.91	3.74	3.54	4.28	1.52
19a	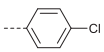	–		27.11	15.95	0.85	32.45	6.85
19b	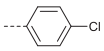	–		3.86	0.83	0.69	1.67	2.72
20a	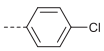	-CH$_2$CH$_2$-		33.37	36.09	3.11	56.82	3.71
5-FU	–	–	–	2.80	0.14	8.81	0.08	0.94

[a] 50% inhibitory concentration or compound concentration required to inhibit tumor cell proliferation by 50%.

direct fusion of benzimidazole to 1,2,3-triazole had detrimental effect on the anti-lung cancer potency. However, benzimidazole directly connected to 1,2,3-triazole contributed to some antitumoral activities. For example, *N*-isopropylamidine **19a** was 6- and 21-fold more active on CFPAC-1 and HeLa cells, respectively, compared to its counterpart **10c** bearing phenoxymethylene linker. Similarly, imidazolino-substituted benzimidazole **19b** displayed 20-fold increased activity on CFPAC-1 cells relative to its structural analog **11c**. Furthermore, the comparison of inhibitory effects between amidine **20a** with ethylene linker and its analog **10c** with phenoxymethylene linker lends support to presumption that ethylene linker has no significant contribution on activities against all evaluated tumor cell lines. However, compounds showing cytostatic activity against cancer cells were also cytotoxic to normal human lung fibroblasts (WI38), although **9c**, **10c**, **11c**, **11f** and **11g** were less cytotoxic (with selectivity index, SI, around 102) compared to other compounds that exhibited antiproliferative effects in submicromolar range, including 5-FU. Some insights into structural requirements including unsubstituted, alkyl-substituted or cyclic amidino moiety at 5-benzimidazole, linkers between 1,2,3-triazole and benzimidazole ring, or 1,2,3-triazole and phenyl ring, as well as type of *p*-substituents at phenyl ring that influenced the cytostatic activities, are presented in Fig. 2.

2.2.2. Apoptosis detection

In order to investigate whether antiproliferative effects of compounds **10c** and **11f** with strong and highly selective activity in non-small cell lung cancer cell line A549 could be associated with induction of apoptosis, Annexin V assay was performed as previously described [33]. Compound **10c** induced marked reduction in viable cell population by 70.59% concomitant with a profound increase in early and late apoptotic/primary necrotic cell populations by 27.81% and 40%, respectively (Table 2, Fig. 3).

Similarly, compound **11f** resulted in a significant decrease in viable cell population by 49.77%, which was accompanied by a marked increase in early and late apoptotic/primary necrotic cell populations by 26.97% and 16.37%, respectively (Table 2, Fig. 3).

2.2.3. Validation of predicted protein targets of compounds *10c* and *11f* by Western blot analysis

In order to further characterize compounds **10c** and **11f** in terms of their mechanism of action and to focus additional biological studies, the Prediction of Activity Spectra for Substances (PASS) [52] was combined with the available literature data for biological activities of structurally related chemical entities and known biological pathways associated with the growth-inhibition effects on A549 cells. Phosphodiesterase 5A (PDE5), cyclin-dependent kinase 9 (CDK9), transglutaminase 2 (TGM2), p38 mitogen-activated protein kinase (p38 MAPK) and sphingosine kinase 1 (SK1) were identified as potential targets of **10c** and **11f** (Table S1, Supplementary information), and their expression levels were analyzed by Western blot (Fig. 4).

PDE5 is cGMP-specific phosphodiesterase that specifically hydrolyzes cGMP to 5′-GMP thereby lowering intracellular cGMP levels. It has been demonstrated that PDE5 is overexpressed in human non-small cell lung tumors compared to normal bronchial epithelium, which suggests that PDE5 plays an important role in lung tumorigenesis [53]. Furthermore, inhibition of PDE5 activity was shown to induce apoptosis in human non-small cell lung cancer cells A549 [53]. Our results showed significant reduction in the expression level of PDE5 in A549 cells treated with compound **11f**, whereas such an effect was not detected with compound **10c**. Thus, PDE5 does not seem to be a putative target of compound **10c**.

Another enzyme that was recognized by PASS as potential target of **11f** was CDK9 which is known to associate with cyclin T1 forming cyclin-dependent kinase pair. Interestingly, it was previously found that CDK9 signaling pathway was related to aberrant transcription profiles observed in lung adenocarcinoma [54]. CDK9 is known to prevent degradation of p53 [55]. Moreover, an overexpression of CDK9 could lead to accumulation of p53 in astroglioma cells pointing to CDK9-dependent regulation of p53 levels. In line with literature data, our results revealed that compound **11f** dramatically reduced the expression level of CDK9/cyclin T1 in A549 cells which was associated with a decline in phospho-p53 (Ser15) levels. On contrary, compound **10c** did not induce marked changes in CDK9/cyclin T1 expression level albeit a trend towards a decrease in phospho-p53 level was observed, suggesting that CDK9/cyclin T1 was not involved in the regulation of p53 activity in the response to treatment with compound **10c**.

TGM2, suggested by *in silico* analyses as a putative target of **10c** and **11f**, is a multi-functional enzyme catalysing the formation of intermolecular isopeptide bonds between glutamine and lysine

Please cite this article in press as: A. Bistrović, et al., Design, synthesis and biological evaluation of novel benzimidazole amidines as potent multi-target inhibitors for the treatment of non-small cell lung cancer, European Journal of Medicinal Chemistry (2017), https://doi.org/10.1016/j.ejmech.2017.10.061

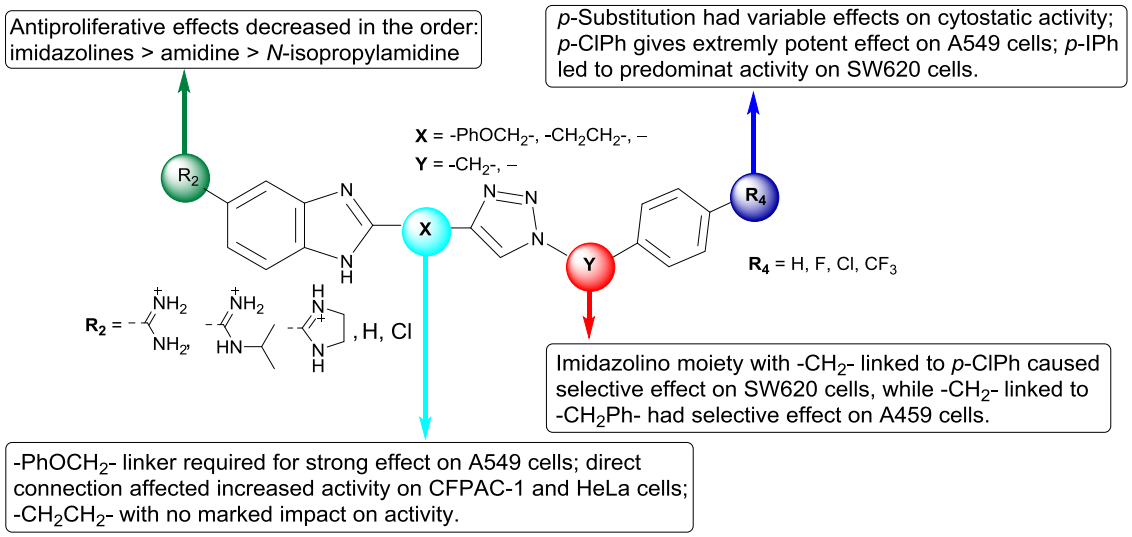

Fig. 2. Structure-activity relationship (SAR) of a series of amidine, *N*-isopropylamidine and imidazoline benzimidazoles coupled with several 1,4-disubstituted 1,2,3-triazolyl moieties.

Table 2
Results of Anexin V assay for apoptosis detection of **10c** and **11f** in A549 cells.

	A549 cells (%)[a]		
	Control	**10c**	**11f**
Secondary necrotic cells	0.00	2.78	6.43
Early apoptotic cells	0.52	28.33	27.49
Viable cells	99.48	28.89	49.71
Late apoptotic/primary necrotic cells	0.00	40.00	16.37

[a] The percentages of viable cells (PI−/Ann V-), early apoptotic cells (PI−/Ann V+), late apoptotic/primary necrotic cells (PI+/Ann V+) and secondary necrotic cells (PI+) after 48 h treatment with compounds **10c** and **11f** at their 2 × IC_{50} values are shown.

side-chains. Importantly, this enzyme has been shown to possess intrinsic serine/threonine kinase activity and to phosphorylate p53 tumor suppressor protein thus regulating its activity [56]. Its expression was previously associated with enhanced invasive and migratory properties of non-small cell lung cancer cells *in vitro* pointing to its tumour-promoting role [57]. Our results showed that TGM2 and phospho-p53 levels were markedly down-regulated upon treatment with **11f**, whereas their expression levels were not significantly altered by compound **10c**.

SK1 catalyses the phosphorylation of sphingosine to form sphingosine-1-phosphate (S1P), a lipid mediator that regulates cell proliferation and survival. Previous findings demonstrated that expression of SK1 was greatly increased in non-small cell lung cancer tissues and cells, and to correlate with tumour progression and poor survival of patients with NSCLC [58,59], which indicates that SK1 may represent a promising pharmacologic target for the treatment of NSCLC. Moreover, several studies provided evidence that SK1 was required for the activation of p38 MAPK in both normal [60] and cancer cells [61]. Similarly, we found that compound **11f** significantly reduced the expression level of phospho-SK1 which was accompanied by a marked decline in phospho-p38 MAPK level (Fig. 4). The same effect was observed with compound **10c** as well, although to a lesser extent. It has been demonstrated that p38 MAPK phosphorylates p53 at serine 15, which seems to be critical for the stabilization, up-regulation, and functional activation of p53 during cellular stress [62]. Further evidence showed that inhibition of p38 precludes stimulation of the transcriptional activity of p53 and that activation of the p38 pathway is sufficient to activate p53 [63]. Taking into account this finding and the abovementioned literature data, we propose that down-regulation of p53 activity in A549 induced by compound **11f** could be associated with abrogation of activities of several kinases including TGM2, CDK9 and p38 MAPK. On the other hand, compound **10c** did not have profound effect on the activities of CDK9 and TGM2, but instead showed moderate downregulation of SK1 activity concomitant with significant reduction in p38 MAPK activity. Since both compounds reduced levels of phospho-p53 although to a different extent, it seems plausible that compounds **10c** and **11f** trigger p53-independent apoptosis. Assuming p38 MAPK as a common biological target for both compounds **10c** and **11f** more detailed structural analysis of possible intramolecular interactions have been investigated.

2.3. Structural analysis of possible interactions of compounds *10c* and *11f* with p38 MAPK

p38 MAPK was selected for further *in silico* molecular binding studies based on our Western blot results revealing marked reduction in its activity induced by both compounds **10c** and **11f**, together with the fact that their structurally related purinomimetic, ralimetinib (LY2228820) [64] found to be a selective inhibitor of p38 MAPK that has been evaluated in clinical trials in patients with advanced cancer. Ralimetinib has shown acceptable safety and pharmacokinetics profiles, which encourages further development of novel p38 MAPK inhibitors in cancer treatment. Here, we analysed the ability of compounds **10c** and **11f** to bind to the ATP-binding site of p38 MAP kinase. Since both compounds incorporate a number of potential pharmacophoric features, their possible interactions with the p38 MAPK active site have been investigated in several steps to elucidate the most probable binding modes. Both structure based-approach in terms of docking to the active site and ligand based approach including field-based alignment were used as described in the methods section.

Due to a large number of available X-ray structures, ligands were grouped into 24 clusters to obtain a representative but chemicaly diverse set for further analysis. Aligned representative structures are shown in Fig. S2, Supplementary data, indicating structural diversity and different binding modes of known inhibitors that fill the ATP-binding region but also hydrophobic regions I and II, as

Please cite this article in press as: A. Bistrović, et al., Design, synthesis and biological evaluation of novel benzimidazole amidines as potent multi-target inhibitors for the treatment of non-small cell lung cancer, European Journal of Medicinal Chemistry (2017), https://doi.org/10.1016/j.ejmech.2017.10.061

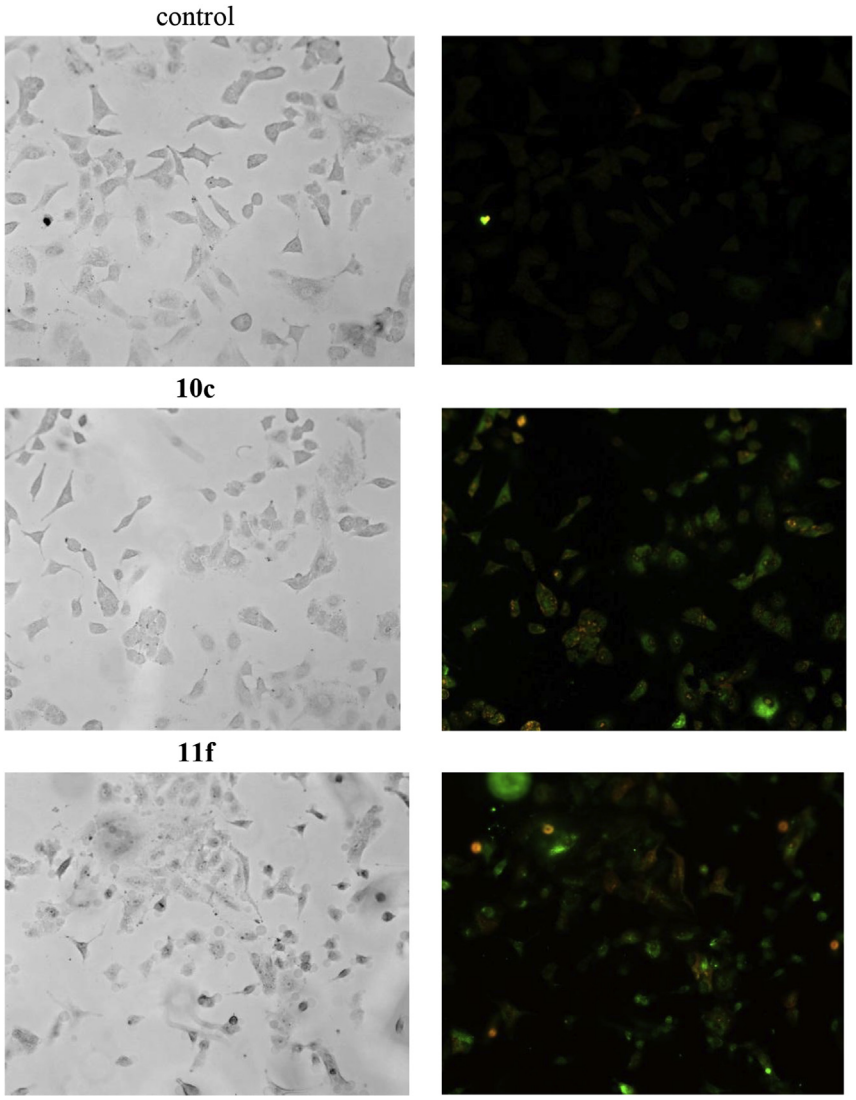

Fig. 3. Detection of apoptosis induced by compounds **10c** and **11f** in non-small cell lung cancer cell line A549 using Annexin V assay. Cells were visualized by fluorescence microscope at 40× magnification before and after treatment with the concentration of 2 × IC_{50} for 48 h. PI staining was used as a nuclear marker. Shown here are bright-field images (left micrographs) and late apoptotic/primary necrotic cells (right micrographs).

well as DFG-out pocket in case of DFG-out inhibitors [65].

Representative ligands were divided into two sets of DFG-in (active form) and DFG-out (in-active form) binders and their structures are shown in Fig. S3 and Fig. S4, Supplementary data. Field-based alignment was performed using bioactive conformations from representative X-ray structures as a reference while structures of **10c** and **11f** were generated from conformational anaylsis. Structures of **10c** and **11f** aligned with the 3LFA ligand, with medium activity of 100 nM, and 3D83 ligand, with strong activity of 8 nM, are presented in Fig. 5. It can be observed that good structural alignment and overlap of major pharmacophoric points have been achieved for both 3LFA and 3D83 reference ligands. Conformations of **10c** and **11f** aligned with representative ligands were sampled for further structural refinement and estimation of binding energies using MM-GBSA method as described below.

The ligand docking studies were carried out with extra precision using the apo-p38 X-ray structure for DFG-in binding mode (pdb:5UOJ) and p38 in complex with a biphenyl amide inhibitor (pdb:3D83) for analysis of DFG-out binding mode. Both unconstrained protocol and protocol with constrained interactions with hinge amino-acids Met109 and Gly110 were applied. In order to explore possible Gyl flip observed for selective p38 inhibitors, 1OVE and 2YIW structures were also used for docking [66,67]. Binding poses of **10c** and **11f** collected from filed-based alignments and from different docking experiments were further refined using Embrace protocol and binding energies were estimated using MM-GBSA protocol as described in the methods section. It was shown previously [68] that the absolute calculated values are not necessarily in agreement with experimental binding affinities. However, the ranking of the ligands based on the calculated binding are expected to correlate with ranking based on experimental binding affinity, particularly in the case of congeneric series. In order to investigate correlation of MM-GBSA calculated binding energies with experimentally determined inhibition, ΔG values for the set of ligands with available X-ray structures and inhibition activities on p38 MAK kinase were calculated. Very good agreement was obtained for a set of 10 inhibitors as shown in Fig. 6. These results indicated that the applied computational strategy could provide plausible ranking of different binding poses for **10c** and **11f** and at least approximate comparison with the activities of known

Please cite this article in press as: A. Bistrović, et al., Design, synthesis and biological evaluation of novel benzimidazole amidines as potent multi-target inhibitors for the treatment of non-small cell lung cancer, European Journal of Medicinal Chemistry (2017), https://doi.org/10.1016/j.ejmech.2017.10.061

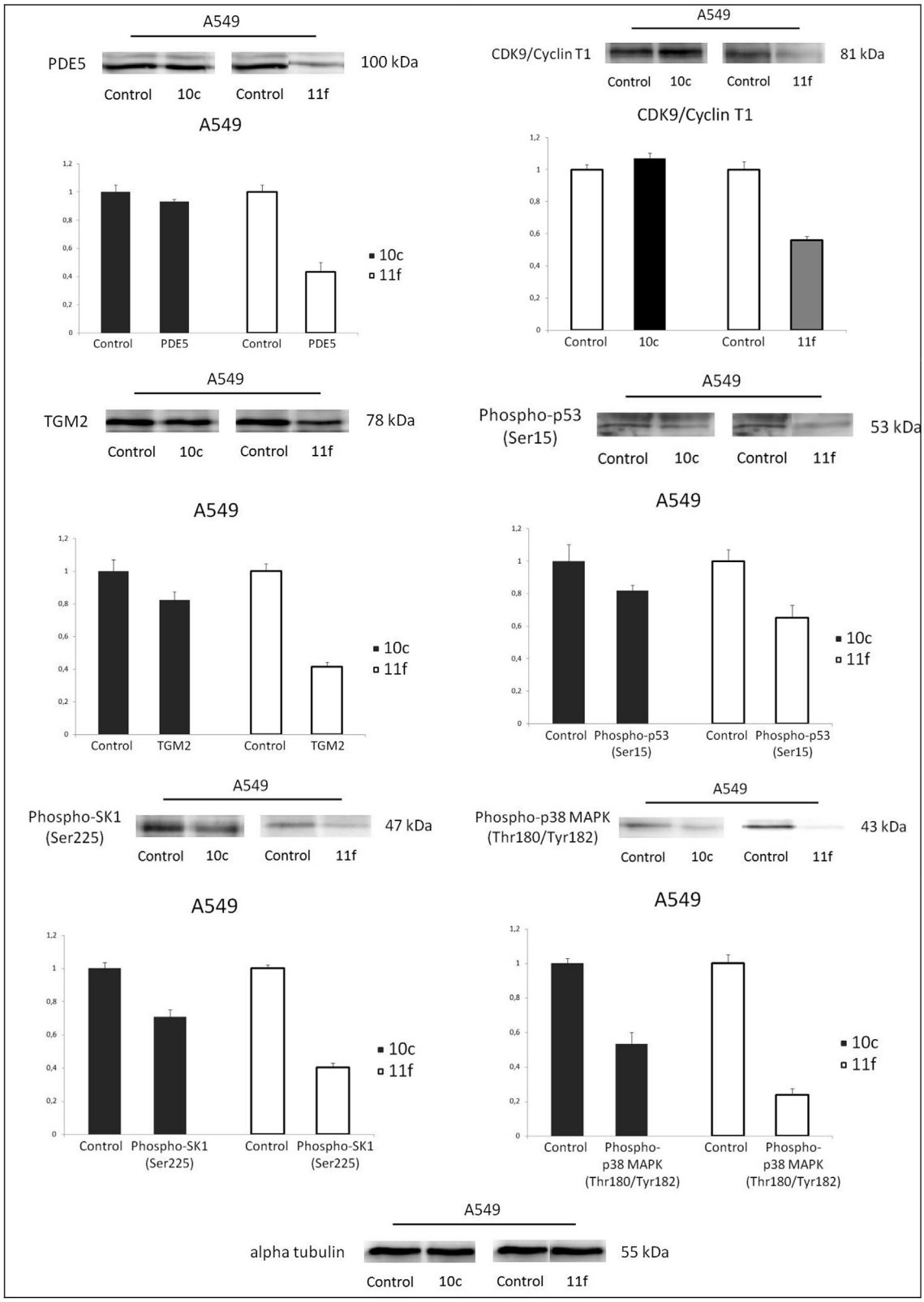

Fig. 4. Western blot analysis of predicted protein targets of compounds **10c** and **11f** in non-small cell lung cancer A549. Representative Western blots are shown detecting the cellular levels of selected proteins before and after treatment of A549 cells with indicated compounds at their 2 × IC_{50} values for 48 h. Approximate molecular weights (kDa) are indicated. Relative protein expressions determined by densitometric analysis of protein bands and normalized to the alpha-tubulin loading control. Two independent experiments were performed with similar results. Data are presented as mean values ± SD. Statistically significant ($p < 0.05$) differences in the expression levels were marked by an asterisk.

Please cite this article in press as: A. Bistrović, et al., Design, synthesis and biological evaluation of novel benzimidazole amidines as potent multi-target inhibitors for the treatment of non-small cell lung cancer, European Journal of Medicinal Chemistry (2017), https://doi.org/10.1016/j.ejmech.2017.10.061

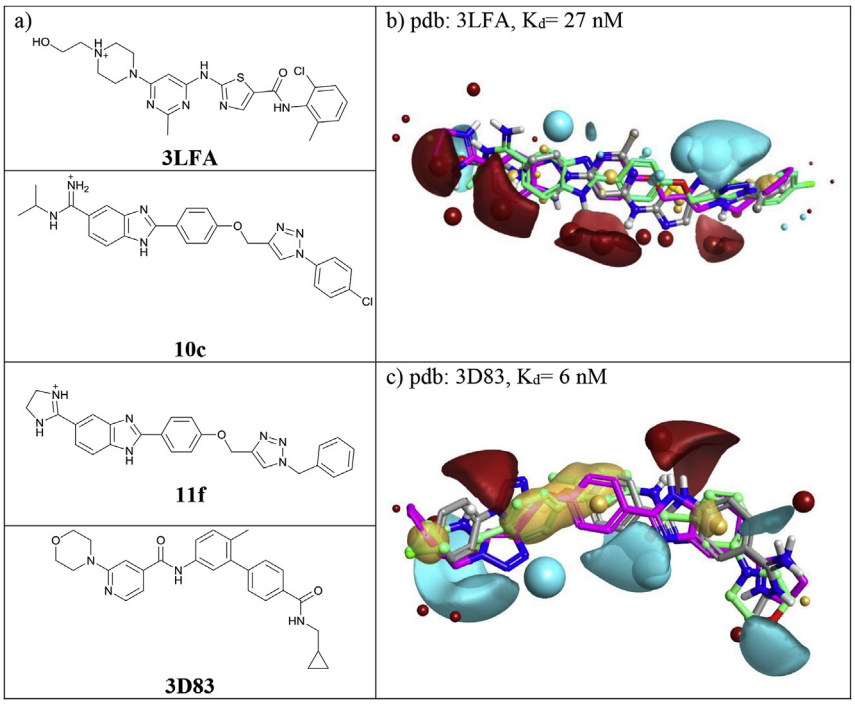

Fig. 5. a) Structures of **10c** and **11f** as well as 3LFA and 3D83 ligands used as a reference structures; b) Field-based alignment of **10c** (green) and **11f** (magenta, spherical fields) with 3LFA ligand (grey, fields as surfaces) and c) Field-based alignment of **10c** (green) and **11f** (magenta, spherical fields) with 3D83 ligand (grey, fields as surfaces). Negative potential fields – blue, positive potential fields – red, hydrophobic fields – yellow. (For interpretation of the references to colour in this figure legend, the reader is referred to the web version of this article.)

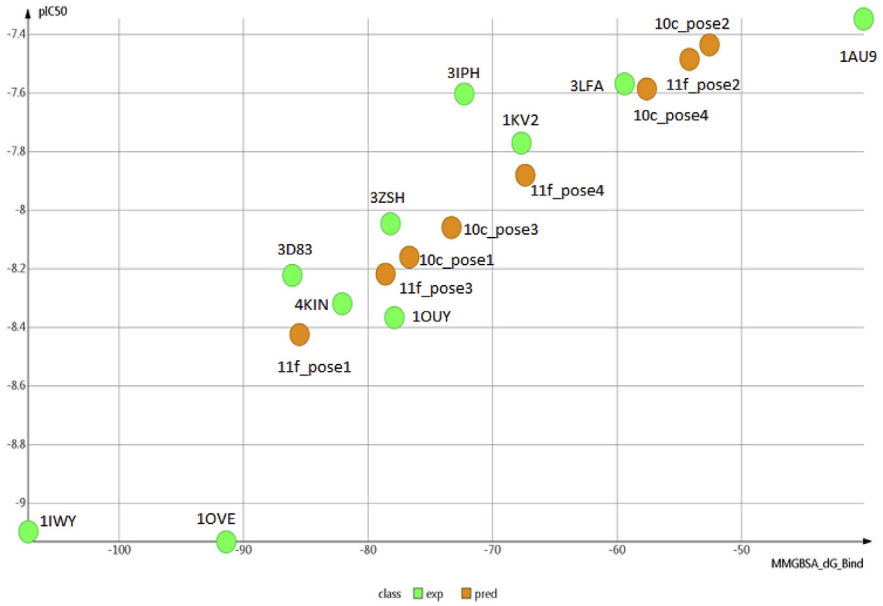

Fig. 6. Correlation between experimental pIC_{50} values and dG values calculated by MMGBSA method for a set of kinase inhibitors (green). Predicted pIC_{50} values for different poses of compounds **10c** and **11f** based on the observed correlation (orange). (For interpretation of the references to colour in this figure legend, the reader is referred to the web version of this article.)

inhibitors. Based on the correlation obtained for the known ligands, inhibitory values are predicted for different binding poses of **10c** and **11f**. Predicted values for different poses all fall in the activity range below 100 nM (Fig. 6.), with DFG-out "3D83-like" binding mode being most active for both compounds; 4 nM for **11f** and 8 nM for **10c**. Compound **11f** is consistently predicted to bind slightly better to p38 MAPK compared to **10c**, which is in good agreement with stronger reduction in the expression level of phospho-p38 MAPK in A549 cells elicited by **11f** (Fig. 4).

Best predicted binding pose of compound **11f** in comparisson with 3D83 ligand is shown in Fig. 7.

The triazole moiety forms an H-bond with the backbone of Met 109 in the hinge region, while the amidino-benzimidazole group forms number of H-bonds with polar amino-acids in the linker

Please cite this article in press as: A. Bistrović, et al., Design, synthesis and biological evaluation of novel benzimidazole amidines as potent multi-target inhibitors for the treatment of non-small cell lung cancer, European Journal of Medicinal Chemistry (2017), https://doi.org/10.1016/j.ejmech.2017.10.061

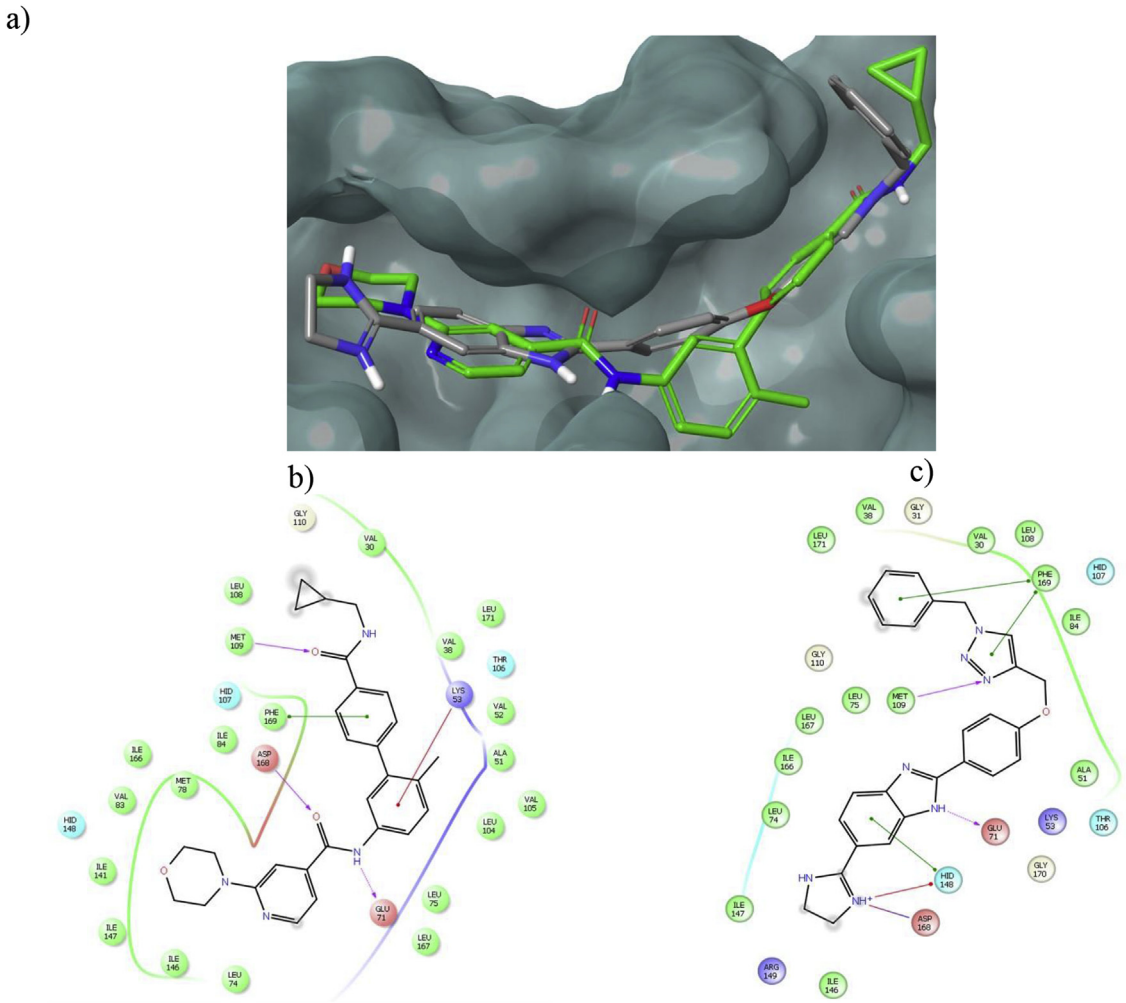

Fig. 7. Best predicted binding pose for compound **11f** obtained from docking, reoptimising 11f-p38 complex with Embrace method and calculating interaction energies using MM-GBSA protocol. a) Overlay of compound **11f** (gray) and 3D83 ligand (green); b) 2D diagram of 3D83-p38 interactions; c) 2D diagram of compound 11f-p38 interactions. (For interpretation of the references to colour in this figure legend, the reader is referred to the web version of this article.)

region; Glu71, Hid148 and Asp168. The phenyl moieties linked to the triazole and benzimidazole are both placed in the hydrophobic environment, the first one forming nice π-π stacking with the Phe169. Other predicted binding poses for compounds **10c** and **11f** are shown in Fig. S5, Supplementary data.

3. Conclusions

Target monocationic and non-cationic benzimidazoles **9a**–**9f**, **10a**–**10g**, **11a**–**11g**, **12c**, **13c**, **19a**, **19b** and **20a** were designed and synthesized by oxidative coupling of *o*-phenylenediamines with benzaldehydes **3a**–**3g** bearing 1,4-disubstituted-1,2,3-triazole that were provided by implementation of environmentally benign synthetic protocols using nonconventional energy sources, microwave and ultrasound irradiation. Compounds **3a**–**3g** were obtained in overall higher yields under ultrasound irradiation compared to reactions performed under microwave irradiation. The present work led to the development of novel *p*-chlorophenyl-substituted 1,2,3-triazolyl *N*-isopropylamidine **10c** and benzyl-substituted 1,2,3-triazolyl imidazoline **11f** benzimidazoles with selective and potent cytostatic activities against non-small cell lung cancer (A549) in the low nM range. Their growth-inhibitory effects on other tested human cancer cell lines including pancreatic adenocarcinoma (CFPAC-1), cervical carcinoma (HeLa) and colorectal adenocarcinoma (SW620) were reduced approximately by two orders of magnitude. Further biological studies of selected candidates **10c** and **11f** revealed that their strong growth inhibitory activity against A549 cells could be associated with induction of apoptosis and primary necrosis. Further analyses provided evidence for different regulation of cellular signalling by **10c** and **11f**. While cytostatic effect of imidazoline benzimidazole **11f** may be ascribed to down-regulation of TGM2, CDK9/cyclin T1, SK1 and particularly p38 MAPK activity, *N*-isopropylamidine benzimidazole **10c** had a profound impact on the activities of only two kinases including SK1 and p38 MAPK, as demonstrated by the reduction in their activities in A549 cells treated with **10c**. Since both compounds inhibited p38 MAPK although with slightly different potency, this enzyme was identified as the common target of **10c** and **11f**. Further *in silico* structural analysis confirmed that both compounds could indeed efficiently inhibit p38 MAP kinase with compound **11f** consistently predicted to bind slightly better to p38 MAPK compared to **10c**, which correlated well with observed stronger decrement in the expression level of phospho-p38 MAPK elicited by **11f** in comparison with **10c**.

Please cite this article in press as: A. Bistrović, et al., Design, synthesis and biological evaluation of novel benzimidazole amidines as potent multi-target inhibitors for the treatment of non-small cell lung cancer, European Journal of Medicinal Chemistry (2017), https://doi.org/10.1016/j.ejmech.2017.10.061

4. Experimentals

4.1. Materials and methods

All solvents were purified following recommended drying agents and/or distilled over 3 Å molecular sieves. For monitoring the progress of a reaction and for comparison purpose, thin layer chromatography (TLC) was performed on pre-coated *Merck* silica gel 60F-254 plates using appropriate solvent system and the spots were detected under UV light (254 nm). For column chromatography silica gel (*Fluka*, 0.063–0.2 mm) was employed, glass column was slurry-packed under gravity. Melting points (uncorrected) were determined with *Kofler* micro hot-stage (*Reichert*, Wien). ^{1}H and ^{13}C NMR spectra were acquired on a *Bruker* 300 and 600 MHz NMR spectrometer as well as 300 MHz Agilent Technologies DD2 NMR spectrometer. All data were recorded in DMSO-d_6 at 298 K. Chemical shifts were referenced to the residual solvent signal of DMSO at δ 2.50 ppm for ^{1}H and δ 39.50 ppm for ^{13}C. Individual resonances were assigned on the basis of their chemical shifts, signal intensities, multiplicity of resonances and H–H coupling constants. High performance liquid chromatography was performed on an *Agilent 1100* series system with UV detection (photodiode array detector) using Zorbax C18 reverse-phase analytical column (2.1 × 30 mm, 3.5 μm). All compounds used for biological evaluation showed >95% purity in this HPLC system. 4800 Plus MALDI TOF/TOF analyzer (Applied Biosystems Inc., Foster City, CA, USA) equipped with a 200 Hz, 355 nm Nd:YAG laser was used for mass accuracy analysis of compounds. Acquisition was performed in positive ion reflector mode. The ultrasound-assisted reactions were carried out in a Bandelin Bath Cleaner (Sonorex digital 10 P) with a nominal power of 1000 W and frequency of 35 kHz. The reactions were carried out in a round-bottomed flask of 25 mL capacity suspended at the centre of the cleaning bath, 5 cm below the surface of the liquid. Microwave-assisted syntheses were performed in a Milestone start S microwave oven using glass cuvettes at 80 °C and 300 W under pressure of 1 bar.

4.2. Experimental procedures for the preparation of compounds

4-(Prop-2-ynyloxy)benzaldehyde (**2**) [69] and amidino substituted *o*-phenylendiamines (**4, 5, 6**) [50] were prepared according to known procedure, while compounds 4-(1,2,3-triazol-4-yl)methoxy)benzaldehydes (**3a, 3b, 3c, 3f**) [70], 4-(1,2,3-triazol-4-yl)methoxy)benzaldehyde (**3g**) [71], (1-(4-chlorophenyl)-1H-1,2,3-triazol-4-yl)methanol (**16**) [72] and 1-(4-chlorophenyl)-1*H*-1,2,3-triazole-4-carbaldehyde (**18**) [72] were synthesized according to modified procedures given in the literature.

4.2.1. General procedure for the synthesis of 4-(1,2,3-triazol-4-yl) methoxy)benzaldehydes (*3a–3g*)

The reaction mixture of compound **2**, Cu(0) (0.8 eq), 1 M $CuSO_4$ (0.3 eq) and the corresponding azide (1.2 eq) was dissolved in 1 mL DMF and a mixture of *t*-BuOH: H_2O = 1: 1 (3 mL). Method A: The reaction mixture was stirred under microwave irradiation (300 W) at 80 °C during 1.5 h. Method B: The reaction mixture was placed in an ultrasonic bath cleaner (1000 W, 35 kHz) at 80 °C for 1.5 h. The solvent was removed under reduced pressure and purified by column chromatography with CH_2Cl_2.

4.2.1.1. 4-((1-Phenyl-1H-1,2,3-triazol-4-yl)methoxy)benzaldehyde (*3a*).

Compound **3a** was prepared using the above mentioned procedure from **2** (200 mg, 1.15 mmol) and azidobenzene (2.76 mL, 1.38 mmol) to obtain **3a** as white solid (Method A: 229.5 mg, 71%; Method B: 310.1 mg, 97%; m.p. = 99–101 °C (m.p. lit. = 101–103 °C) [70]. ^{1}H NMR (600 MHz, DMSO) δ 9.89 (1H, s, COH), 8.99 (1H, s, H5′), 7.93–7.89 (4H, m, Ph), 7.61 (2H, t, J = 7.9 Hz, Ph), 7.51 (1H, t, J = 7.5 Hz, Ph), 7.29 (2H, d, J = 8.7 Hz, Ph), 5.38 (2H, s, OCH_2).^{13}C NMR (75 MHz, DMSO) δ 191.63, 163.01, 143.37, 136.62, 132.01, 130.12, 129.05, 123.32, 120.38, 115.40, 61.46.

4.2.1.2. 4-((1-(4-Fluorophenyl)-1H-1,2,3-triazol-4-yl)methoxy)benzaldehyde (*3b*).

Compound **3b** was prepared using the above mentioned procedure from **2** (200 mg, 1.15 mmol) and 1-azido-4-fluorobenzene (2.76 mL, 1.38 mmol). After purification by column chromatography compound **3b** was isolated as white powder (Method A: 161.1 mg, 47%; Method B: 325.6 mg, 95%; m.p. = 140–142 °C, m.p. lit. = 138–140 °C) [70]. ^{1}H NMR (300 MHz, DMSO) δ 9.89 (1H, s, CHO), 8.96 (1H, s, H5′), 8.00–7.85 (4H, m, Ph), 7.47 (2H, t, J = 8.8 Hz, Ph), 7.28 (2H, d, J = 8.7 Hz, Ph), 5.38 (2H, s, OCH_2). ^{13}C NMR (75 MHz, DMSO) δ 191.49, 163.44; 160.18 (d, J_{CF} = 248.8 Hz), 162.92, 143.32, 133.15; 133.11 (d, J_{CF} = 2.9 Hz), 131.91, 130.03, 123.49, 122.76, 122.65, (d, J_{CF} = 8.8 Hz), 117.01, 116.70 (d, J_{CF} = 23.2 Hz), 115.32, 61.40.

4.2.1.3. 4-((1-(4-Chlorophenyl)-1H-1,2,3-triazol-4-yl)methoxy)benzaldehyde (*3c*).

Compound **3c** was prepared using the above mentioned procedure from **2** (200 mg, 1.15 mmol) and 1-azido-4-chlorobenzene (2.76 mL, 1.38 mmol). After purification by column chromatography compound **3c** was isolated as white powder (Method A: 122.3 mg, 34%; Method B: 224.2 mg, 62%; m.p. = 151–154 °C, m.p. lit. = 151–153 °C) [70]. ^{1}H NMR (600 MHz, DMSO) δ 9.89 (1H, s, CHO), 9.01 (1H, s, H5′), 7.96 (2H, d, J = 8.8 Hz, Ph), 7.90 (2H, d, J = 8.7 Hz, Ph), 7.69 (2H, d, J = 8.8 Hz, Ph), 7.28 (2H, d, J = 8.7 Hz, Ph), 5.38 (2H, s, OCH_2).^{13}C NMR (151 MHz, DMSO) δ 191.44, 162.87, 143.45, 135.34, 133.18, 131.87, 130.02, 129.94, 123.28, 121.98, 115.30, 61.37.

4.2.1.4. 4-((1-(4-Iodophenyl)-1H-1,2,3-triazol-4-yl)methoxy)benzaldehyde (*3d*).

Compound **3d** was prepared using the above mentioned procedure from **2** (200 mg, 1.15 mmol) and 1-azido-4-iodobenzene (2.76 mL, 1.38 mmol After purification by column chromatography compound **3d** was obtained as white powder (Method A: 270.6 mg, 56%; Method B: 381.7 mg, 82%; m.p. = 259–262 °C). ^{1}H NMR (600 MHz, DMSO) δ 9.89 (1H, s, COH), 9.01 (1H, s, H5′), 7.97 (2H, d, J = 8.7 Hz, Ph), 7.90 (2H, d, J = 8.7 Hz, Ph), 7.74 (2H, d, J = 8.7 Hz, Ph), 7.28 (2H, d, J = 8.7 Hz, Ph), 5.38 (2H, s, OCH_2). ^{13}C NMR (151 MHz, DMSO) δ 191.67, 163.00, 143.59, 138.84, 136.32, 132.04, 130.13, 123.25, 122.34, 115.43, 94.63, 61.43.

4.2.1.5. 4-((1-(4-(Trifluoromethyl)phenyl)-1H-1,2,3-triazol-4-yl) methoxy)benzaldehyde (*3e*).

Compound **3e** was prepared using the above mentioned procedure from **2** (200 mg, 1.15 mmol) and 1-azido-4-(trifluoromethyl)benzene (2.76 mL, 1.38 mmol). After purification by column chromatography compound **3e** was isolated as white powder (Method A: 120.4 mg, 30%; Method B: 396.3 mg, 99%; m.p. = 251–253 °C). ^{1}H NMR (600 MHz, DMSO) δ 9.90 (1H, s, CHO), 9.14 (1H, s, H5′), 8.19 (2H, d, J = 8.5 Hz, Ph), 8.01 (2H, d, J = 8.6 Hz, Ph), 7.91 (2H, d, J = 8.7 Hz, Ph), 7.29 (2H, d, J = 8.7 Hz, Ph), 5.41 (2H, s, OCH_2). ^{13}C NMR (151 MHz, DMSO) δ 191.57, 162.93, 143.77, 131.97, 130.12, 129.32; 129.11; 128.89; 128.70 (q, J_{CF} = 32.4 Hz), 127.40; 127.38; 127.36; 127.33 (q, J_{CF} = 3.5 Hz), 124.80; 123.00 (d, J_{CF} = 271.4 Hz), 123.53, 120.86, 115.38, 61.38.

4.2.1.6. 4-((1-Benzyl-1H-1,2,3-triazol-4-yl)methoxy)benzaldehyde (*3f*).

Compound **3f** was prepared using the above mentioned procedure from **2** (200 mg, 1.15 mmol) and benzyl azide (2.76 mL, 1.38 mmol). After purification by column chromatography **3f** was obtained as white solid (Method A: 239.1 mg, 71%; Method B: 303.6 mg, 90%; m.p. = 101–103 °C, m.p. lit. = 99–100 °C) [70]. ^{1}H NMR (300 MHz, DMSO) δ 9.88 (1H, s, CHO), 8.33 (1H, s, H5′), 7.87

Please cite this article in press as: A. Bistrović, et al., Design, synthesis and biological evaluation of novel benzimidazole amidines as potent multi-target inhibitors for the treatment of non-small cell lung cancer, European Journal of Medicinal Chemistry (2017), https://doi.org/10.1016/j.ejmech.2017.10.061

(2H, d, $J = 8.7$ Hz, Ph), 7.44–7.27 (5H, m, Ph), 7.23 (2H, d, $J = 8.7$ Hz, Ph), 5.62 (2H, s, CH_2), 5.27 (2H, s, CH_2). ^{13}C NMR (75 MHz, DMSO) δ 191.32, 162.91, 142.32, 135.94, 131.75, 129.84, 128.76, 128.16, 127.96, 124.94, 115.19, 61.42, 52.84. MS (*m/z*) 294.1 $[M+H]^+$.

*4.2.1.7. 4-((1-(4-Chlorobenzyl)-1H-1,2,3-triazol-4-yl)methoxy)benzaldehyde (**3g**).* Compound **3g** was prepared using the above mentioned procedure from **2** (200 mg, 1.15 mmol) and *p*-chlorobenzyl azide (2.76 mL, 1.38 mmol). After purification by column chromatography **3g** was obtained as white powder (Method B: 302.2 mg, 80%; m.p. = 106–108 °C, m.p. lit. = 108–111 °C) [71]. ^{1}H NMR (600 MHz, DMSO) δ 9.88 (1H, s, CHO), 8.33 (1H, s, H5′), 7.87 (2H, d, $J = 8.7$ Hz, Ph), 7.45 (2H, d, $J = 8.4$ Hz, Ph), 7.35 (2H, d, $J = 8.4$ Hz, Ph), 7.23 (2H, d, $J = 8.7$ Hz, Ph), 5.63 (2H, s, CH_2), 5.27 (2H, s, CH_2). ^{13}C NMR (75 MHz, DMSO) δ 191.33, 162.90, 142.38, 134.92, 132.90, 131.76, 129.93, 129.86, 128.77, 124.98, 115.19, 61.41, 52.04.MS (*m/z*) 328.1 $[M+H]^+$.

*4.2.2. General procedure for the synthesis of 5-amidino-2-phenyl benzimidazoles (**9a**–**9f**, **10a**–**10g** and **11a**–**11g**)*

The reaction mixture of 4-triazolylbenzaldehyde derivatives (**3a**–**g**), *o*-phenylenediamine (**4**, **5** or **6**) and 40% $NaHSO_3$ (aq) was dissolved in 15 mL EtOH and stirred under reflux for 6–8 h. After completition of the reaction $NaHSO_3$ was filtered and the reaction mixture was evaporated to dryness. Water was added (5 mL) and the mixture was stirred over night and filtered. The crude residue was dissolved in HCl saturated EtOH (8–10 mL) and stirred over night. Addition of ether resulted in precipitation of products **9a**–**9f, 10a**–**10g** and **11a**–**11g**. Solid was collected by filtration, washed with anhydrous ether, and dried under vacuum.

*4.2.2.1. 2-(4-((1-Phenyl-1H-1,2,3-triazol-4-yl)methoxy)phenyl)-1H-benzo[d]imidazole-5-carboximidamide hydrochloride (**9a**).* Compound **9a** was prepared using the above described method from **3a** (200 mg, 0.72 mmol) and *o*-phenylenediamine **4** (113.4 mg, 0.64 mmol) to obtain **9a** as brown powder (100.3 mg, 28%, m.p. = 159–162 °C). ^{1}H NMR (300 MHz, DMSO) δ 9.42 (2H, bs, NH), 9.13–8.99 (3H, m, NH, H5′), 8.33 (2H, d, $J = 8.8$ Hz, Ph), 8.18 (1H, s, H4), 7.92 (2H, d, $J = 7.6$ Hz, Ph), 7.86 (1H, d, $J = 8.5$ Hz, H7), 7.76 (1H, dd, $J = 8.6$, 1.4 Hz, H6), 7.62 (2H, t, $J = 7.7$ Hz, Ph), 7.56–7.45 (1H, m, Ph), 7.37 (2H, d, $J = 8.9$ Hz, Ph), 5.40 (2H, s, CH_2).^{13}C NMR (151 MHz, DMSO) δ 165.45, 162.11, 151.80, 143.22, 136.56, 136.20, 132.72, 130.57, 130.03, 128.95, 124.96, 124.56, 123.34, 120.29, 116.18, 116.00, 114.71, 114.33, 61.52. Anal. calcd. for $C_{23}H_{19}N_7O$ x 2 HCl x 5 H_2O (*Mr* = 572.45): C 48.26, H 5.46, N 17.13; found: C 48.53, H 5.76, N 17.28%. HRMS: calcd. for $C_{23}H_{19}N_7O$ $(M + H)^+$: 410.1729; found: 410.1740.

*4.2.2.2. 2-(4-((1-(4-Fluorophenyl)-1H-1,2,3-triazol-4-yl)methoxy)phenyl)-1H-benzo[d]imidazole-5-carboximidamide hydrochloride (**9b**).* Compound **9b** was prepared using the above described method from **3b** (200 mg, 0.67 mmol) and *o*-phenylenediamine **4** (101.0 mg, 0.67 mmol) to obtain **9b** as brown powder (87 mg, 27%, m.p. = 218–220 °C). ^{1}H NMR (300 MHz, DMSO) δ 9.37 (2H, bs, NH), 9.02–8.94 (3H, m, NH, H5′), 8.28 (2H, d, $J = 8.7$ Hz, Ph), 8.15 (1H, s, H4), 7.90 (2H, d, $J = 8.7$ Hz, Ph), 7.83 (1H, d, $J = 8.4$ Hz, H7), 7.72 (1H, d, $J = 8.0$ Hz, H6), 7.35 (2H, d, $J = 8.9$ Hz, Ph), 7.28 (2H, d, $J = 8.7$ Hz, Ph), 5.38 (2H, s, CH_2). ^{13}C NMR (75 MHz, DMSO) δ 165.84, 163.34; 160.08 (d, $J_{CF} = 245.8$ Hz), 162.83, 153.50, 143.42, 143.23, 133.07, 131.81, 129.95, 129.22, 123.43, 122.66; 122.54 (d, $J_{CF} = 8.8$ Hz), 116.61; 116.92 (d, $J_{CF} = 23.3$ Hz), 115.48, 115.24, 61.35. Anal. calcd. for $C_{23}H_{18}FN_7O$ x 2 HCl x 3 H_2O (*Mr* = 554.41): C 49.83, H 4.73, N 17.68; found: C 49.82, H 4.78, N 17.54%. HRMS: calcd. for $C_{23}H_{18}FN_7O$ $(M + H)^+$: 428.1635; found: 428.1619.

*4.2.2.3. 2-(4-((1-(4-Chlorophenyl)-1H-1,2,3-triazol-4-yl)methoxy)phenyl)-1H-benzo[d]imidazole-5-carboximidamide hydrochloride (**9c**).* Compound **9c** was prepared using the above described method from **3c** (200 mg, 0.64 mmol) and *o*-phenylenediamine **4** (86.5 mg, 0.58 mmol) to give **9c** as brown powder (142.1 mg, 41%, m.p. = 212–213 °C). ^{1}H NMR (300 MHz, DMSO) δ 9.53 (2H, bs, NH), 9.22 (2H, bs, NH), 9.07 (1H, s, H5′), 8.45 (2H, d, $J = 8.9$ Hz, Ph), 8.23 (1H, s, H4), 7.98 (2H, d, $J = 8.9$ Hz, Ph), 7.91 (1H, d, $J = 8.5$ Hz, H7), 7.83 (1H, dd, $J = 8.6$, 1.4 Hz, H6), 7.69 (2H, d, $J = 8.9$ Hz, Ph), 7.40 (2H, d, $J = 8.9$ Hz, Ph), 5.42 (2H, s, CH_2).^{13}C NMR (75 MHz, DMSO) δ 165.60, 161.40, 152.38, 143.41, 135.31, 133.10, 130.02, 129.89, 123.99, 123.46, 123.30, 121.89, 115.70, 115.01, 114.28, 61.35. Anal. calcd. for $C_{23}H_{18}ClN_7O$ x 2 HCl x 2.6 H_2O (*Mr* = 536.66): C 49.01, H 4.51, N 17.39; found: C 49.33, H 4.27, N 17.48%. HRMS: calcd. for $C_{23}H_{18}ClN_7O$ $(M + H)^+$: 444.1340; found: 444.1346.

*4.2.2.4. 2-(4-((1-(4-Iodophenyl)-1H-1,2,3-triazol-4-yl)methoxy)phenyl)-1H-benzo[d]imidazole-5-carboximidamide hydrochloride (**9d**).* Compound **9d** was prepared using the above described method from **3d** (100 mg, 0.25 mmol) and *o*-phenylenediamine **4** (37.06 mg, 0.25 mmol) to obtain red powder **9d** (63.2 mg, 42%, m.p. = 229–231 °C). ^{1}H NMR (300 MHz, DMSO) δ 9.41 (2H, bs, NH), 9.05 (3H, bs, NH, H5′), 8.32 (2H, d, $J = 8.5$ Hz, Ph), 8.17 (1H, s, H4), 7.98 (1H, d, $J = 8.6$ Hz, H7), 7.79–7.73 (3H, m, H6, Ph), 7.36 (2H, d, $J = 8.8$ Hz, Ph), 5.39 (2H, s, OCH_2).^{13}C NMR (75 MHz, DMSO) δ 165.70 (CNH), 160.87, 153.14, 143.52, 138.62, 136.16, 129.97, 129.48, 123.18, 123.07, 122.57, 122.06, 115.80, 115.57, 94.54, 61.27. Anal. calcd. for $C_{23}H_{18}N_7IO$ x 2 HCl x 3.75 H_2O (*Mr* = 675.82): C 40.88, H 4.10, N 14.51; found: 40.64, H 3.96, N 14.78%. HRMS: calcd. for $C_{23}H_{18}N_7IO$ $(M + H)^+$: 536.0696; found: 536.0679.

*4.2.2.5. 2-(4-((1-(4-(Trifluoromethyl)phenyl)-1H-1,2,3-triazol-4-yl)methoxy)phenyl)-1H-benzo[d]imidazole-5-carboximidamide hydrochloride (**9e**).* Compound **9e** was prepared using the above described method from **3e** (200 mg, 0.58 mmol) and *o*-phenylenediamine **4** (86.5 mg, 0.58 mmol) and to obtain **3e** as grey solid (144.0 mg, 39%, m.p. = 247–250 °C). ^{1}H NMR (300 MHz, DMSO) δ 9.43 (2H, bs, NH), 9.18 (1H, s, H5′) 9.07 (2H, bs, NH), 8.35 (2H, d, $J = 8.9$ Hz, Ph), 8.26–8.14 (3H, m, H4, Ph), 8.02 (2H, d, $J = 8.8$ Hz, Ph), 7.88 (1H, $J = 8.7$ Hz, H7), 7.78 (1H, dd, $J = 8.5$, 1.6 Hz, H6), 7.39 (2H, d, $J = 8.9$ Hz, Ph), 5.44 (2H, s, OCH_2). ^{13}C NMR (75 MHz, DMSO) δ 166.02, 160.91, 153.73, 144.04, 140.38, 139.48, 137.43, 130.04, 129.78; 129.35; 128.92; 128.91 (q, $J_{CF} = 32.4$ Hz), 129.50, 127.59, 127.54; 127.50; 127.45 (q, $J_{CF} = 3.7$ Hz), 127.45, 125.81; 122.21 (d, $J_{CF} = 272$ Hz), 123.64, 123.22, 122.59, 120.98, 120.16, 115.84, 114.73, 61.38. Anal. calcd. for $C_{24}H_{18}F_3N_7O$ x 2 HCl x 2.6 H_2O (*Mr* = 597.21): C 48.27, H 4.25, N 16.42; found: 48.52, H 4.32, N 16.18%. HRMS: calcd. for $C_{24}H_{18}F_3N_7O$ $(M + H)^+$: 478.1603; found: 478.1611.

*4.2.2.6. 2-(4-((1-Benzyl-1H-1,2,3-triazol-4-yl)methoxy)phenyl)-1H-benzo[d]imidazole-5-carboximidamide hydrochloride (**9f**).* Compound **9f** was prepared using the above described method from **3f** (90 mg, 0.31 mmol) and *o*-phenylenediamine **4** (46.56 mg, 0.31 mmol) to obtain **9f** as grey powder (140.6 mg, 90%, m.p. = 204–206 °C). ^{1}H NMR (300 MHz, DMSO) δ 9.48 (2H, s, NH), 9.12 (2H, s, NH), 8.40–8.32 (3H, m H5′, Ph), 8.20 (1H, s, H4), 7.89 (1H, d, $J = 8.5$ Hz, H7), 7.80 (1H, dd, 1H, $J = 8.6$ Hz, H6), 7.47–7.27 (7H, m, Ph), 5.64 (2H, s, CH_2), 5.30 (2H, s, CH_2).^{13}C NMR (75 MHz, DMSO) δ 166.27, 161.19, 153.97, 142.94, 140.49, 137.57, 136.19, 129.61, 129.27, 128.74, 128.43, 125.37, 123.43, 122.83, 120.07, 116.01, 115.93, 114.95, 61.63, 53.39. Anal. calcd. for $C_{24}H_{21}N_7O$ x 2 HCl x 0.3 H_2O (*Mr* = 501.80): C 47.44, H 4.74, N 19.54; found: 47.71, H 4.58, N 19.27%. HRMS: calcd. for $C_{24}H_{21}N_7O$ $(M + H)^+$: 424.1886; found: 424.1881.

Please cite this article in press as: A. Bistrović, et al., Design, synthesis and biological evaluation of novel benzimidazole amidines as potent multi-target inhibitors for the treatment of non-small cell lung cancer, European Journal of Medicinal Chemistry (2017), https://doi.org/10.1016/j.ejmech.2017.10.061

*4.2.2.7. N-Isopropyl-2-(4-((1-phenyl-1H-1,2,3-triazol-4-yl)methoxy) phenyl)-1H-benzo[d]imidazole-5-carboximidamide hydrochloride (**10a**).* Compound **10a** was prepared using the above described method from **3a** (200 mg, 0.72 mmol) and *o*-phenylenediamine **5** (114.2 mg, 0.72 mmol) to obtain **10a** as brown powder (144.5 mg, 34%, m.p. = 194–197 °C). ^{1}H NMR (300 MHz, DMSO) δ 9.65 (1H, d, *J* = 7.8 Hz, NH), 9.50 (1H, s, NH), 9.10–9.01 (2H, m, NH, H5′), 8.38 (2H, d, *J* = 8.5 Hz, Ph), 8.08 (1H, s, H4), 7.99–7.82 (3H, m, H7, Ph), 7.56–7.48 (1H, m, H6), 7.39 (2H, d, *J* = 8.7 Hz, Ph), 5.41 (2H, s, OCH_2), 4.22–3.97 (1H, m, CH), 1.31 (6H, d, *J* = 6.2 Hz, $\underline{CH_3}C\underline{CH_3}$).^{13}C NMR (75 MHz, DMSO) δ 162.81, 160.88, 153.96, 143.85, 140.65, 138.07, 136.81, 130.46, 129.43, 123.87, 123.55, 123.27, 120.84, 120.65, 116.01, 114.86, 61.52, 45.54, 21.58. Anal. calcd. for $C_{26}H_{25}N_7O$ x 2 HCl x 3.75 H_2O (*Mr* = 592.01): C 52.75, H 5.87, N 16.56; found: 52.78, H 5.72, N 16.50%. HRMS: calcd. for $C_{26}H_{25}N_7O$ $(M + H)^+$: 452.2199; found: 452.2202.

*4.2.2.8. 2-(4-((1-(4-Fluorophenyl)-1H-1,2,3-triazol-4-yl)methoxy) phenyl)-N-isopropyl-1H-benzo[d]imidazole-5-carboximidamide hydrochloride (**10b**).* Compound **10b** was prepared using the above described method from **3b** (200 mg, 0.67 mmol) and *o*-phenylenediamine **5** (119.2 mg, 0.67 mmol) to obtain **10b** as white powder (243.7 mg, 60%, m.p. = 214–216 °C). ^{1}H NMR (300 MHz, DMSO) δ 9.65 (1H, d, *J* = 7.6 Hz, NH), 9.50 (1H, s, NH), 9.07 (1H, s, NH), 9.01 (1H, s, H5′), 8.38 (2H, d, *J* = 8.6 Hz, Ph), 8.08 (1H, s, H4), 8.02–7.93 (2H, m, Ph), 7.87 (1H, d, *J* = 8.5 Hz, H7), 7.67 (1H, dd, *J* = 8.5, 1.1 Hz, H6), 7.48 (2H, t, *J* = 8.8 Hz, Ph), 7.38 (2H, d, *J* = 8.8 Hz, Ph), 5.40 (2H, s, OCH_2), 4.31–3.94 (1H, m, CH), 1.32 (6H, d, *J* = 6.3 Hz, $\underline{CH_3}C\underline{CH_3}$). ^{13}C NMR (75 MHz, DMSO) δ 163.47; 160.21 (d, J_{CF} = 245.9 Hz), 162.21, 160.99, 153.03, 143.48, 133.18; 133.14 (d, J_{CF} = 2.9 Hz), 130.09, 129.55, 124.12, 123.53, 122.79; 122.67 (d, J_{CF} = 8.8 Hz), 119.45, 117.06; 116.75 (d, J_{CF} = 23.3 Hz), 115.74, 115.49, 114.41, 61.36, 45.21, 21.35. Anal. calcd. for $C_{26}H_{24}FN_7O$ x 2 HCl x 3.5 H_2O (*Mr* = 605.40): C 51.57, H 5.49, N 16.19; found: C 51.57, H 5.24, N 16.48%. HRMS: calcd. for $C_{26}H_{24}FN_7O$ $(M + H)^+$: 470.2105; found: 470.2082.

*4.2.2.9. 2-(4-((1-(4-Chlorophenyl)-1H-1,2,3-triazol-4-yl)methoxy) phenyl)-N-isopropyl-1H-benzo[d]imidazole-5-carboximidamide hydrochloride (**10c**).* Compound **10c** was prepared using the above described method from **3c** (200 mg, 0.64 mmol) and *o*-phenylenediamine **5** (113.4 mg, 0.64 mmol) to obtain **10c** as brown powder (92.7 mg, 25%, m.p. = 218–220 °C). ^{1}H NMR (300 MHz, DMSO) δ 9.65 (1H, d, *J* = 7.8 Hz, NH), 9.50 (1H, s, NH), 9.07 (2H, s, NH and H5′), 8.38 (2H, d, *J* = 8.6 Hz, Ph), 8.08 (1H, s, H4), 7.98 (2H, d, *J* = 8.8 Hz, Ph), 7.87 (1H, d, *J* = 8.4 Hz, H7), 7.73–7.64 (3H, m, H6, Ph), 7.37 (2H, d, *J* = 8.8 Hz, Ph), 5.40 (2H, s, OCH_2), 4.16–3.95 (1H, m, CH), 1.31 (6H, d, *J* = 6.3 Hz, $\underline{CH_3}C\underline{CH_3}$).^{13}C NMR (75 MHz, DMSO) δ 161.95, 161.10, 152.53, 143.46, 135.31, 133.10, 129.90, 129.72, 126.48, 124.35, 123.82, 123.29, 121.89, 116.35, 61.30, 45.10, 21.26. Anal. calcd. for $C_{26}H_{24}ClN_7O$ x 2 HCl x 0.75 H_2O (*Mr* = 572.41): C 54.56, H 4.84, N 17.13; found: C 54.25, H 4.92, N 17.16%. HRMS: calcd. for $C_{26}H_{24}ClN_7O$ $(M + H)^+$: 486.1809; found: 486.1818.

*4.2.2.10. 2-(4-((1-(4-Iodophenyl)-1H-1,2,3-triazol-4-yl)methoxy) phenyl)-N-isopropyl-1H-benzo[d]imidazole-5-carboximidamide hydrochloride (**10d**).* Compound **10d** was prepared using the above described method from **3d** (200 mg, 0.49 mmol) and *o*-phenylenediamine **5** (86.8 mg, 0.49 mmol) to obtain **10d** as brown powder (93.2 mg, 28%, m.p. = 219–221 °C). ^{1}H NMR (300 MHz, DMSO) δ 9.70 (1H, d, *J* = 7.6 Hz, NH), 9.55 (1H, s, NH), 9.16 (1H, s, NH), 9.07 (1H, s, H5′), 8.46 (2H, d, *J* = 8.6 Hz, Ph), 8.09 (1H, s, H4), 7.97 (2H, d, *J* = 8.7 Hz, Ph), 7.88 (1H, d, *J* = 8.5 Hz, H7), 7.79–7.67 (3H, m, H6, Ph), 7.38 (2H, d, *J* = 8.8 Hz, Ph), 5.40 (2H, s, CH_2), 4.18–4.06 (1H, m, CH), 1.31 (6H, d, *J* = 6.3 Hz, $\underline{CH_3}C\underline{CH_3}$).^{13}C NMR (151 MHz, DMSO) δ 162.18, 161.05, 152.95, 147.73, 143.61, 142.84, 138.75, 136.25, 131.12, 129.59, 124.25, 123.67, 123.17, 122.21, 115.76, 114.38, 94.60, 61.35, 45.21, 21.32. Anal. calcd. for $C_{26}H_{24}IN_7O$ x 2 HCl x 1.3 H_2O (*Mr* = 673.77): C 46.35, H 4.28, N 14.55; found: C 46.68, H 4.33, N 14.84%. HRMS: calcd. for $C_{26}H_{24}IN_7O$ $(M + H)^+$: 578.1165; found: 578.1140.

*4.2.2.11. N-Isopropyl-2-(4-((1-(4-(trifluoromethyl)phenyl)-1H-1,2,3-triazol-4-yl)methoxy)phenyl)-1H-benzo[d]imidazole-5-carboximidamide hydrochloride (**10e**).* Compound **10e** was prepared using the above described method from **3e** (200 mg, 0.58 mmol) and *o*-phenylenediamine **5** (78.1 mg, 0.52 mmol) to obtain **8e** as brown powder (139.4 mg, 34%, m.p. = 204–206 °C). ^{1}H NMR (300 MHz, DMSO) δ 9.69 (1H, d, *J* = 7.7 Hz, NH), 9.53 (1H, s, NH), 9.20 (1H, s, H5′), 9.11 (1H, s, NH), 8.43 (2H, d, *J* = 8.6 Hz, Ph), 8.20 (2H, d, *J* = 8.4 Hz, Ph), 8.09 (1H, s, H4), 8.01 (2H, d, *J* = 8.5 Hz, Ph), 7.89 (1H, d, *J* = 8.5 Hz, H7), 7.70 (1H, d, *J* = 8.4 Hz, H6), 7.40 (2H, d, *J* = 8.7 Hz, Ph), 5.44 (2H, s, CH_2), 4.17–4.03 (1H, m, CH), 1.31 (6H, d, *J* = 6.3 Hz, $\underline{CH_3}C\underline{CH_3}$).^{13}C NMR (75 MHz, DMSO) δ 162.51, 160.80, 153.58, 144.05, 140.13, 139.48, 137.46, 132.13, 129.38, 129.07; 128.92; 128.49; 128.22 (q, J_{CF} = 33.0 Hz), 127.60; 127.55; 127.50; 127.45 (q, J_{CF} = 3.8 Hz), 125.81; 122.20 (d, J_{CF} = 272.4 Hz) 123.84, 123.63, 123.28, 120.97, 120.42, 115.83, 114.61, 61.36, 45.33, 21.45. Anal. calcd. for $C_{27}H_{24}F_3N_7O$ x 2 HCl x 3.75 H_2O (*Mr* = 696.47): C 49.47, H 5.07, N 14.96; found: C 49.56, H 4.99, N 14.88%. HRMS: calcd. for $C_{27}H_{24}F_3N_7O$ $(M + H)^+$: 520.2073; found: 520.2059.

*4.2.2.12. N-Isopropyl-2-(4-((1-benzyl-1H-1,2,3-triazol-4-yl) methoxy)phenyl)-1H-benzo[d]imidazole-5-carboximidamide hydrochloride (**10f**).* Compound **10f** was prepared using the above described method from **3f** (200 mg, 0.68 mmol) and *o*-phenylenediamine **5** (120.5 mg, 0.68 mmol) to obtain **10f** as brown powder (195.9 mg, 53%, m.p. = 198–201 °C). ^{1}H NMR (600 MHz, DMSO) δ 9.75 (1H, d, *J* = 7.7 Hz, NH), 9.59 (1H, s, NH), 9.21 (1H, s, NH), 8.51 (2H, d, *J* = 8.5 Hz, Ph), 8.37 (1H, s, H5′), 8.12 (1H, d, *J* = 0.9 Hz, H4), 7.90 (1H, d, *J* = 8.5 Hz, H7), 7.74 (1H, dd, *J* = 8.3, 1.1 Hz, H6), 7.40–7.32 (7H, m, Ph), 5.64 (2H, s, CH_2), 5.31 (2H, s, CH_2), 4.17–4.10 (1H, m, CH), 1.31 (6H, d, *J* = 6.4 Hz, $\underline{CH_3}C\underline{CH_3}$).^{13}C NMR (75 MHz, DMSO) δ 165.63, 161.85, 152.32, 147.18, 145.76, 142.39, 142.36, 135.95, 129.81, 129.71, 128.77, 128.17, 127.98, 124.97, 124.58, 124.04, 115.62, 114.17, 61.41, 52.85, 45.12, 21.25. Anal. calcd. for $C_{27}H_{27}N_7O$ x 2 HCl x 0.2 H_2O (*Mr* = 542.08): C 59.82, H 5.47, N 18.09; found: C 59.81, H 5.79, N 18.41%. HRMS: calcd. for $C_{27}H_{27}N_7O$ $(M + H)^+$: 466.2355; found: 466.2374.

*4.2.2.13. N-Isopropyl-2-(4-((1-(4-chlorobenzyl)-1H-1,2,3-triazol-4-yl)methoxy)phenyl)-1H-benzo[d]imidazole-5-carboximidamide hydrochloride (**10g**).* Compound **10g** was prepared using the above described method from **3g** (200 mg, 0.61 mmol) and *o*-phenylenediamine **5** (117.32 mg, 0.61 mmol) to obtain **10g** as white powder (184.6 mg, 53%, m.p. = 183–186 °C). ^{1}H NMR (300 MHz, DMSO) δ 9.84 (1H, d, *J* = 7.8 Hz, NH), 9.67 (1H, s, NH), 9.30 (1H, s, NH), 8.60 (2H, d, *J* = 8.8 Hz, Ph), 8.40 (1H, s, H5′), 8.15 (1H, s, H4), 7.96 (1H, d, *J* = 8.5 Hz, H7), 7.80 (1H, dd, *J* = 8.5, 1.0 Hz, H6), 7.45 (2H, d, *J* = 8.4 Hz, Ph), 7.41–7.30 (4H, m, Ph), 5.65 (2H, s, CH_2), 5.33 (2H, s, CH_2), 4.22–4.07 (1H, m, CH), 1.31 (6H, d, *J* = 6.3 Hz, $\underline{CH_3}C\underline{CH_3}$).^{13}C NMR (75 MHz, DMSO) δ 162.18, 161.50, 151.06, 142.28, 135.19, 134.94, 132.90, 131.94, 130.68, 129.98, 128.78, 125.88, 125.36, 125.13, 115.82, 115.64, 114.52, 113.93, 61.52, 52.05, 45.26, 21.25. Anal. calcd. for $C_{27}H_{26}ClN_7O$ x 2 HCl x 0.2 H_2O (*Mr* = 576.53): C 56.25, H 4.97, N 17.00; found: C 56.21, H 4.16, N 16.88%. HRMS: calcd. for $C_{27}H_{26}ClN_7O$ $(M + H)^+$: 500.1966; found: 500.1956.

4.2.2.14. 5-(4,5-Dihydro-1H-imidazol-2-yl)-2-(4-((1-phenyl-1H-1,2,3-triazol-4-yl)methoxy)phenyl)-1H-benzo[d]imidazole

Please cite this article in press as: A. Bistrović, et al., Design, synthesis and biological evaluation of novel benzimidazole amidines as potent multi-target inhibitors for the treatment of non-small cell lung cancer, European Journal of Medicinal Chemistry (2017), https://doi.org/10.1016/j.ejmech.2017.10.061

*hydrochloride (**11a**).* Compound **11a** was prepared using the above described method from **3a** (200 mg, 0.72 mmol) and *o*-phenylenediamine **6** (127.6 mg, 0.64 mmol) to obtain **11a** as white powder (199.6 mg, 50%, m.p. = 171–173 °C). 1H NMR (600 MHz, DMSO) δ 10.69 (2H, s, NH), 9.02 (1H, s, H5′), 8.38 (1H, s, H4), 8.33 (2H, d, *J* = 8.5 Hz, Ph), 7.94–7.86 (4H, m, H6, H7 and Ph), 7.62 (2H, t, *J* = 7.8 Hz, Ph), 7.52 (1H, t, *J* = 7.4 Hz, Ph), 7.36 (2H, d, *J* = 8.7 Hz, Ph), 5.40 (2H, s, OCH_2), 4.03 (4H, s, $\underline{CH_2}\underline{CH_2}$). ^{13}C NMR (151 MHz, DMSO) δ 165.12, 160.80, 153.69, 143.34, 138.43, 137.80, 136.50, 129.89, 129.45, 128.79, 123.30, 123.11, 121.39, 120.17, 116.35, 115.51, 115.46, 114.92, 61.30, 44.28. Anal. calcd. for $C_{25}H_{21}N_7O$ x 2 HCl x 2.5 H_2O (*Mr* = 553.45): C 54.25, H 5.10, N 17.72; found: 54.71, H 4.95, N 17.62%. HRMS: calcd. for $C_{25}H_{21}N_7O$ $(M + H)^+$: 436.1886; found: 436.1880.

*4.2.2.15. 5-(4,5-Dihydro-1H-imidazol-2-yl)-2-(4-((1-(4-fluorophenyl)-1H-1,2,3-triazol-4-yl)methoxy)phenyl)-1H-benzo[d]imidazole hydrochloride (**11b**).* Compound **11b** was prepared using the above described method from **3b** (200 mg, 0.67 mmol) and **6** (106.87 mg, 0.60 mmol) to obtain **11b** as brown powder (103.3 mg, 27%, m.p. = 215–218 °C). ^{1}H NMR (600 MHz, DMSO) δ 10.74 (2H, s, NH), 9.00 (1H, s, H5′), 8.40 (1H, s, H4), 8.36 (2H, d, *J* = 8.6 Hz, Ph), 8.00–7.92 (3H, m, H7, Ph), 7.89 (1H, d, *J* = 8.5 Hz, H6), 7.47 (2H, t, *J* = 8.7 Hz, Ph), 7.36 (2H, d, *J* = 8.7 Hz, Ph), 5.39 (2H, s, CH_2), 4.03 (4H, s, $\underline{CH_2}\underline{CH_2}$).^{13}C NMR (75 MHz, DMSO) δ 165.41, 163.41, 160.15, d, J_{CF} = 245.9 Hz), 160.54, 154.25, 143.51, 143.29, 134.22, 133.15; 133.11 (d, J_{CF} = 2.9 Hz), 129.59, 129.17, 123.42, 122.84, 122.72; 122.60 (d, J_{CF} = 8.8 Hz), 120.76, 116.99; 116.68 (d, J_{CF} = 23.3 Hz), 116.18, 115.87, 115.53, 61.28, 44.35. Anal. calcd. for $C_{25}H_{20}FN_7O$ x 2 HCl x 1.7 H_2O (*Mr* = 563.66): C 59.91, H 4.60, N 17.60; found: C 59.73, H 4.66, N 17.93%. HRMS: calcd. for $C_{25}H_{20}FN_7O$ $(M + H)^+$: 454.1792; found: 454.1805.

*4.2.2.16. 2-(4-((1-(4-Chlorophenyl)-1H-1,2,3-triazol-4-yl)methoxy)phenyl)-5-(4,5-dihydro-1H-imidazol-2-yl)-1H-benzo[d]imidazole hydrochloride (**11c**).* Compound **11c** was prepared using the above described method from **3c** (200 mg, 0.64 mmol) and **6** (112.98 mg, 0.64 mmol) to obtain **11c** as brown powder (227.3 mg, 63%, m.p. = 207–209 °C). ^{1}H NMR (300 MHz, DMSO) δ 10.77 (s, 1H), 9.06 (s, 1H), 8.42 (s, 1H), 8.37 (d, *J* = 8.7 Hz, 1H), 8.03–7.92 (m, *J* = 10.4, 7.3 Hz, 3H), 7.69 (d, *J* = 8.8 Hz, 2H), 7.38 (d, *J* = 8.7 Hz, 1H), 5.40 (s, 1H), 4.04 (s, 2H).^{13}C NMR (75 MHz, DMSO) δ 165.47, 160.44, 154.37, 143.68, 135.37, 133.78, 133.37, 133.19, 131.90, 129.98, 129.10, 123.27, 122.72, 121.97, 121.04, 115.74, 115.52, 115.31, 61.25, 44.35. Anal. calcd. for $C_{25}H_{20}ClN_7O$ x 2 HCl x 1.3 H_2O (*Mr* = 566.27): C 53.03, H 4.38, N 17.31; found: C 52.82, H 4.33, N 17.33%. HRMS: calcd. for $C_{25}H_{20}ClN_7O$ $(M + H)^+$: 470.1496; found: 470.1492.

*4.2.2.17. 5-(4,5-Dihydro-1H-imidazol-2-yl)-2-(4-((1-(4-iodophenyl)-1H-1,2,3-triazol-4-yl)methoxy)phenyl)-1H-benzo[d]imidazole hydrochloride (**11d**).* Compound **11d** was prepared using the above described method from **3d** (200 mg, 0.49 mmol) and **6** (87.5 mg, 0.49 mmol to obtain **11d** as brown powder (95.0 mg, 28%, m.p. = 152–154 °C). ^{1}H NMR (600 MHz, DMSO) δ 10.67 (2H, s, NH), 9.04 (1H, s, H5′), 8.37 (1H, s, H4), 8.31 (2H, d, *J* = 8.6 Hz, Ph), 7.97 (2H, d, *J* = 8.6 Hz, Ph), 7.90 (1H, d, *J* = 8.1 Hz, H7), 7.85 (1H, d, *J* = 8.4 Hz, H6), 7.75 (2H, d, *J* = 8.6 Hz, Ph), 7.34 (2H, d, *J* = 8.7 Hz, Ph), 5.38 (2H, s, CH_2), 4.03 (4H, s, $\underline{CH_2}\underline{CH_2}$). ^{13}C NMR (75 MHz, DMSO) δ 165.17, 160.58, 153.89, 143.56, 138.60, 136.15, 129.29, 128.42, 126.56, 123.04, 122.04, 120.87, 116.04, 115.45, 94.52, 61.23, 44.27. Anal. calcd. for $C_{25}H_{20}IN_7O$ x 2 HCl x 1.9 H_2O (*Mr* = 688.53): C 44.91, H 3.89, N 14.66; found: C 45.18, H 3.93, N 14.82%. HRMS: calcd. for $C_{25}H_{20}IN_7O$ $(M + H)^+$: 562.0852; found: 562.0850.

*4.2.2.18. 5-(4,5-Dihydro-1H-imidazol-2-yl)-2-(4-((1-(4-(trifluoromethyl)phenyl)-1H-1,2,3-triazol-4-yl)methoxy)phenyl)-1H-benzo[d]imidazole hydrochloride (**11e**).* Compound **11e** was prepared using the above described method from **3e** (200 mg, 0.58 mmol) and **6** (92.2 mg, 0.52 mmol) to obtain **11e** as white powder (77.4 mg, 22%, m.p. = 169–171 °C). ^{1}H NMR (300 MHz, DMSO) δ 10.50 (2H, s, NH), 9.17 (1H, s, H5′), 8.32–8.18 (5H, m, H4, Ph), 8.02 (2H, d, *J* = 8.7 Hz, Ph), 7.83 (2H, s, H7 and H6), 7.34 (2H, d, *J* = 8.9 Hz, Ph), 5.41 (2H, s, OCH_2), 4.05 (4H, s, $\underline{CH_2}\underline{CH_2}$). ^{13}C NMR (151 MHz, DMSO) δ 165.12, 160.71, 153.74, 143.77, 139.27, 138.56, 135.63, 131.77, 129.42, 129.10; 128.88; 128.67; 128.45 (q, J_{CF} = 32.4 Hz), 127.24; 127.22; 127.19; 127.17 (q, J_{CF} = 3.5 Hz), 124.66; 122.86 (d, J_{CF} = 272.4 Hz), 123.38, 123.26, 121.04, 120.65, 116.28, 115.50, 115.22, 61.22, 44.28. Anal. calcd. for $C_{26}H_{20}F_3N_7O$ x 2 HCl x 2 H_2O (*Mr* = 612.44): C 50.99, H 4.28, N 16.01; found: 51.13, H 4.21, N 15.87%. HRMS: calcd. for $C_{26}H_{20}F_3N_7O$ $(M + H)^+$: 504.1760; found: 504.1741.

*4.2.2.19. 2-(4-((1-Benzyl-1H-1,2,3-triazol-4-yl)methoxy)phenyl)-5-(4,5-dihydro-1H-imidazol-2-yl)-1H-benzo[d]imidazole hydrochloride (**11f**).* Compound **11f** was prepared using the above described method from **3f** (125 mg, 0.43 mmol) and **6** (70.9 mg, 0.40 mmol) to obtain **11f** as brown powder (130.2 mg, 51%, m.p. = 198–201 °C). 1H NMR (600 MHz, DMSO) δ 10.92 (2H, s, NH), 8.49 (1H, s, H5′), 8.44 (2H, d, *J* = 8.5 Hz, Ph), 8.38 (1H, s, H4), 8.04 (1H, d, *J* = 8.3 Hz, H7), 7.96 (1H, d, *J* = 8.5 Hz, H6), 7.41–7.32 (7H, m, Ph), 5.64 (2H, s, CH_2), 5.31 (2H, s, CH_2), 4.04 (4H, s, $\underline{CH_2}\underline{CH_2}$). ^{13}C NMR (75 MHz, DMSO) δ 165.03, 161.48, 153.21, 142.49, 139.07, 136.02, 135.62, 129.93, 128.89, 128.31, 128.09, 125.08, 124.13, 118.25, 117.30, 115.73, 114.81, 61.50, 52.98, 44.46. Anal. calcd. for $C_{26}H_{23}N_7O$ x 2 HCl x 2.4 H_2O (*Mr* = 594.93): C 55.21, H 5.31, N 17.33; found: C 52.13, H 4.99, N 17.58%. HRMS: calcd. for $C_{26}H_{23}N_7O$ $(M + H)^+$: 405.2042; found: 405.2029.

*4.2.2.20. 2-(4-((1-(4-Chlorobenzyl)-1H-1,2,3-triazol-4-yl)methoxy)phenyl)-5-(4,5-dihydro-1H-imidazol-2-yl)-1H-benzo[d]imidazole hydrochloride (**11g**).* Compound **11g** was prepared using the above described method from **3g** (200 mg, 0.61 mmol) and **6** (139.52 mg, 0.61 mmol) to obtain **11g** as white powder (321.3 mg, 92%, m.p. > 250 °C). ^{1}H NMR (600 MHz, DMSO) δ 10.89 (2H, s, NH), 8.47 (1H, s, H5′), 8.42 (2H, d, *J* = 8.2 Hz, Ph), 8.38 (1H, s, H4), 8.02 (d, *J* = 8.2 Hz, 1H), 7.92 (d, *J* = 8.3 Hz, 1H), 7.45 (d, *J* = 8.0 Hz, 1H), 7.36 (d, *J* = 8.0 Hz, 1H), 7.33 (d, *J* = 8.4 Hz, 1H), 5.64 (s, 2H), 5.30 (s, 1H), 4.03 (s, 4H).^{13}C NMR (75 MHz, DMSO) δ 187.52, 165.05, 161.09, 153.47, 142.52, 135.50, 134.96, 134.46, 132.92, 129.98, 129.63, 128.80, 126.27, 125.03, 123.65, 116.73, 115.56, 114.77, 110.63, 61.39, 52.07, 44.34. Anal. calcd. for $C_{26}H_{22}ClN_7O$ x 2 HCl x 0.7 H_2O (*Mr* = 569.49): C 54.84, H 4.49, N 17.22; found: C 55.09, H 4.20, N 17.28%. HRMS: calcd. for $C_{26}H_{22}ClN_7O$ $(M + H)^+$: 484.1653; found: 484.1638.

*4.2.3. General procedure for the synthesis of compounds **12c** and **13c***

The reaction mixture of 4-triazolylbenzaldehyde derivative (**3c**), *o*-phenylenediamine (**7 or 8**) and 40% $NaHSO_3$ was dissolved in 15 mL EtOH and stirred under reflux for 6–8 h. After completition of the reaction $NaHSO_3$ was filtered and the reaction mixture was evaporated to dryness. Water was added (5 mL) and the mixture was stirred over night and filtered. The crude residue was dissolved in acetone addition of water resulted in precipitation of products **12c** and **13c**.

*4.2.3.1. 2-(4-((1-(4-Chlorophenyl)-1H-1,2,3-triazol-4-yl)methoxy)phenyl)-1H-benzo[d]imidazole (**12c**).* Compound **12c** was prepared using the above described method from **3c** (200 mg, 0.64 mmol) and **7** (69.21 mg, 0.64 mmol) to obtain **12c** as white crystals

Please cite this article in press as: A. Bistrović, et al., Design, synthesis and biological evaluation of novel benzimidazole amidines as potent multi-target inhibitors for the treatment of non-small cell lung cancer, European Journal of Medicinal Chemistry (2017), https://doi.org/10.1016/j.ejmech.2017.10.061

(205.8 mg, 80%, m.p. > 250 °C). ^{1}H NMR (300 MHz, DMSO) δ 12.76 (1H, s, NH), 9.03 (1H, s, H5′), 8.14 (2H, d, *J* = 8.8 Hz, Ph), 7.97 (2H, d, *J* = 8.8 Hz, Ph), 7.69 (2H, d, *J* = 8.8 Hz, Ph), 7.60–7.52 (2H, m, H5, H6), 7.26 (2H, d, *J* = 8.8 Hz, Ph), 7.21–7.14 (2H, m, H4, H7), 5.34 (2H, s, CH_2).^{13}C NMR (75 MHz, DMSO) δ 159.27, 151.20, 143.80, 135.34, 133.06, 129.88, 128.02, 123.14, 123.10, 121.87, 121.79, 115.15, 61.12. Anal. calcd. for $C_{22}H_{16}ClN_5O$ x 2.6 H_2O (*Mr* = 448.69): C 58.89, H 4.76, N 15.61; found: C 58.62, H 4.55, N 15.67%. HRMS: calcd. for $C_{22}H_{16}ClN_5O$ $(M + H)^+$: 402.1122; found: 402.1134.

*4.2.3.2. 5-Chloro-2-(4-((1-(4-chlorophenyl)-1H-1,2,3-triazol-4-yl) methoxy)phenyl)-1H-benzo[d]imidazole (**13c**).* Compound **13c** was prepared using the above described method from **3c** (200 mg, 0.64 mmol) and **7** (90.90 mg, 0.64 mmol) to obtain **13c** as light brown powder (185 mg, 66%, m.p. > 250 °C) ^{1}H NMR (600 MHz, DMSO) δ 12.96 (1H, bs, NH), 9.01 (1H, s, H5′), 8.13 (2H, d, *J* = 8.6 Hz, Ph), 7.97 (2H, d, *J* = 8.7 Hz, Ph), 7.68 (2H, d, *J* = 8.7 Hz, Ph), 7.60 (1H, s, H4), 7.56 (1H, d, *J* = 8.2 Hz, H7), 7.27 (2H, d, *J* = 8.6 Hz, Ph), 7.20 (1H, dd, *J* = 8.6, 1.3 Hz, H6), 5.35 (2H, s, CH_2).^{13}C NMR (151 MHz, DMSO) δ 159.54, 152.60, 143.73, 135.31, 133.05, 129.84, 128.21, 126.10, 123.07, 122.54, 122.01, 121.84, 115.21, 61.14. Anal. calcd. for $C_{22}H_{15}Cl_2N_5O$ x 0.6 H_2O (*Mr* = 476.21): C 59.10, H 3.65, N 15.66; found: C 58.95, H 3.55, N 15.63%. HRMS: calcd. for $C_{22}H_{15}Cl_2N_5O$ $(M + H)^+$: 436.0732; found: 436.0743.

*4.2.4. General procedure for the synthesis of 1-(4-chlorophenyl)-1,2,3-triazolyl alcohols **15** and **16***

1-Azido-4-chlorobenzene (1 eq), the corresponding terminal alkyne (propargyl alcohol or 4-pentyn-1-ol, 1 eq) and $Cu(OAc)_2$ (0.05 eq) were dissolved in methanol. The reaction mixture was placed in an ultrasonic bath cleaner (1000 W, 35 kHz) at 55 °C for 1.5 h. The solvent was removed under reduced pressure and purified by column chromatography with CH_2Cl_2: MeOH = 50: 1.

*4.2.4.1. (1-(4-Chlorophenyl)-1H-1,2,3-triazol-4-yl)methanol (**15**).* Compound **15** was prepared using the above mentioned procedure from propargyl alcohol (0.07 mL, 1.2 mmol) and 1-azido-4-chlorobenzene (2.76 mL, 1.2 mmol). After purification by column chromatography **15** was obtained as white powder (184.4 mg, 88%; m.p. = 145–146 °C). ^{1}H NMR (300 MHz, DMSO) δ 8.71 (1H, s, H5′), 7.95 (2H, d, *J* = 8.9 Hz, Ph), 7.66 (2H, d, *J* = 8.9 Hz, Ph), 5.34 (1H, t, *J* = 5.6 Hz, OH), 4.61 (2H, d, *J* = 5.5 Hz, $\underline{CH_2}OH$).^{13}C NMR (75 MHz, DMSO) δ 149.30, 135.53, 132.71, 129.83, 121.59, 121.06, 54.91. MS (*m/z*) 210.0 $[M+H]^+$.

*4.2.4.2. 3-(1-(4-Chlorophenyl)-1H-1,2,3-triazol-4-yl)propan-1-ol (**16**).* Compound **16** was prepared using the above mentioned procedure from 4-pentyn-1-ol (0.11 mL, 1.2 mmol) and 1-azido-4-chlorobenzene (2.76 mL, 1.38 mmol). After purification by column chromatography **16** was obtained as white powder (235 mg, 99%; m.p. = 96–99 °C). ^{1}H NMR (300 MHz, DMSO) δ 8.60 (1H, s, H5′), 7.92 (2H, d, *J* = 8.9 Hz, Ph), 7.66 (2H, d, *J* = 8.9 Hz, Ph), 4.53 (1H, t, *J* = 5.1 Hz, OH), 3.48 (2H, dd, *J* = 11.6, 6.2 Hz, $CH_2CH_2\underline{CH_2}OH$), 2.74 (2H, t, *J* = 7.7 Hz, $\underline{CH_2}CH_2CH_2OH$), 1.93–1.71 (1H, m, $CH_2\underline{CH_2}CH_2OH$).^{13}C NMR (75 MHz, DMSO) δ 148.24, 135.59, 132.51, 129.80, 121.41, 120.18, 59.96, 32.02, 21.63. MS (*m/z*) 238.1 $[M+H]^+$.

*4.2.5. General procedure for the synthesis of 1-(4-chlorophenyl)-1,2,3-triazolyl aldehydes **17** and **18***

DMSO (8 mmol) was added dropwise to a solution of oxalyl chloride (4 mmol) in CH_2Cl_2 (4 mL) at −78 °C. After 2 min, a solution of the corresponding 1,2,3-triazolyl alcohol **15** or **16** (1 mmol) in 0.11 mL CH_2Cl_2 was added slowly over 5 min. After stirring for an additional 15 min Et_3N (8 mmol) was added to the reaction mixture and stirred at −78 °C for 5 min and then the mixture was warmed to room temperature. The reaction mixture was diluted with EtOAc, washed with water and brine. The combined extracts were dried over $MgSO_4$, filtered, concentrated and purified by column chromatography with CH_2Cl_2:CH_3OH = 50:1 [51].

*4.2.5.1. 1-(4-Chlorophenyl)-1H-1,2,3-triazole-4-carbaldehyde (**17**).* Compound **17** was prepared using the above mentioned procedure from **15** (165 mg, 0.79 mmol). After purification by column chromatography **17** was obtained as white powder (101.5 mg, 62%; m.p. = 165–169 °C). ^{1}H NMR (300 MHz, DMSO) δ 10.12 (1H, s, CHO), 9.60 (1H, s, H5′), 8.03 (2H, d, *J* = 8.9 Hz, Ph), 7.73 (2H, d, *J* = 8.9 Hz, Ph).^{13}C NMR (75 MHz, DMSO) δ 184.97, 147.59, 134.79, 133.89, 129.94, 126.30, 122.47. MS (*m/z*) 208.0 $[M+H]^+$.

*4.2.5.2. 3-(1-(4-Chlorophenyl)-1H-1,2,3-triazol-4-yl)propanal (**18**).* Compound **18** was prepared using the above mentioned procedure from **16** (150 mg, 0.63 mmol). After purification by column chromatography **17** was obtained as white powder (96.1 mg, 65%; m.p. = 57–62 °C). ^{1}H NMR (600 MHz, DMSO) δ 9.77 (1H, s, CHO), 8.60 (1H, s, H5′), 7.90 (2H, d, *J* = 8.8 Hz, Ph), 7.66 (2H, d, *J* = 8.9 Hz, Ph), 2.98 (1H, t, *J* = 7.1 Hz, CH_2), 2.89 (2H, t, *J* = 7.2 Hz, CH_2).^{13}C NMR (75 MHz, DMSzzO) δ 202.36, 147.03, 135.50, 132.63, 129.83, 121.45, 120.43, 41.81, 17.85. MS (*m/z*) 236.0 $[M+H]^+$.

*4.2.6. General procedure for the synthesis of compounds **19a**, **19b** and **20a***

The reaction mixture 1-(4-chlorophenyl)-1*H*-1,2,3-triazol-4-yl) aldehyde derivatives (**17 or 18**), *o*-phenylenediamine (**5** or **6**) and 40% $NaHSO_3$ was dissolved in 15 mL EtOH and stirred under reflux for 6–8 h. After completition of the reaction $NaHSO_3$ was filtered and the reaction mixture was evaporated to dryness. Water was added (5 mL) and the mixture was stirred over night and filtered. The crude residue was dissolved in HCl saturated EtOH (8–10 mL) and stirred over night. Addition of ether resulted in precipitation of products **19a, 19b** and **20a** Solid was collected by filtration, washed with anhydrous ether, and dried under vacuum.

*4.2.6.1. 2-(1-(4-Chlorophenyl)-1H-1,2,3-triazol-4-yl)-N-isopropyl-1H-benzo[d]imidazole-5-carboximidamide hydrochloride (**19a**).* Compound **19a** was prepared using the above described method from **17** (200 mg, 0.96 mmol) and **5** (204.87 mg, 0.96 mmol) to obtain **19a** as brown powder (280.7 mg, 77%, m.p. > 250 °C). ^{1}H NMR (300 MHz, DMSO) δ 9.67 (1H, s, NH), 9.56 (1H, d, *J* = 8.2 Hz, NH), 9.41 (1H, s, NH), 9.02 (1H, s, H5′), 8.15–7.97 (3H, m, H4, Ph), 7.84–7.69 (3H, m, Ph, H7), 7.59 (1H, d, *J* = 8.8 Hz, H6), 4.24–3.90 (1H, m, CH), 1.31 (6H, d, *J* = 5.8 Hz, $\underline{CH_3}C\underline{CH_3}$).^{13}C NMR (75 MHz, DMSO) δ 162.39, 146.62, 139.75, 135.07, 133.58, 129.95, 123.37, 123.10, 122.50, 122.25, 45.00, 21.29. Anal. calcd. for $C_{19}H_{18}ClN_7$ x 2 HCl x 5.2 H_2O (*Mr* = 546.45): C 41.76, H 5.61, N 17.94; found: C 42.00, H 5.24, N 17.88%. HRMS: calcd. for $C_{19}H_{18}ClN_7$ $(M + H)^+$: 380.1390; found: 380.1375.

*4.2.6.2. 2-(1-(4-Chlorophenyl)-1H-1,2,3-triazol-4-yl)-5-(4,5-dihydro-1H-imidazol-2-yl)-1H-benzo[d]imidazole hydrochloride (**19b**).* Compound **19b** was prepared using the above described method from **17** (150 mg, 0.72 mmol) and **6** (165.24 mg, 0.72 mmol) to obtain **19b** as brown powder (135 mg, 52%, m.p. > 250 °C). ^{1}H NMR (300 MHz, DMSO) δ 10.62 (2H, s, NH), 9.70 (1H, s, H5′), 8.39 (1H, bs, H4), 8.10 (2H, d, *J* = 7.4 Hz, Ph), 7.93–7.68 (4H, m, H6, H7, Ph), 4.03 (4H, s,CH_2CH_2).^{13}C NMR (75 MHz, DMSO) δ 165.39, 139.70, 135.06, 133.60, 129.97, 129.82, 123.52, 122.68, 122.20, 121.77, 115.69, 44.26. Anal. calcd. for $C_{18}H_{14}ClN_7$ x 2 HCl x 7 H_2O (*Mr* = 562.84): C 38.41, H 5.37, N 17.40; found: C 38.37, H 5.25, N 17.64%. HRMS: calcd. for $C_{18}H_{14}ClN_7$ $(M + H)^+$: 364.1077; found: 364.1083.

Please cite this article in press as: A. Bistrović, et al., Design, synthesis and biological evaluation of novel benzimidazole amidines as potent multi-target inhibitors for the treatment of non-small cell lung cancer, European Journal of Medicinal Chemistry (2017), https://doi.org/10.1016/j.ejmech.2017.10.061

*4.2.6.3. 2-(2-(1-(4-Chlorophenyl)-1H-1,2,3-triazol-4-yl)ethyl)-N-isopropyl-1H-benzo[d]imidazole-5-carboximidamide hydrochloride (**20a**).* Compound **20a** was prepared using the above described method from **18** (180 mg, 0.76 mmol) and **5** (162.44 mg, 0.76 mmol) to obtain **20a** as white powder (150.3 mg, 48%, m.p. = 199–201 °C). ^{1}H NMR (600 MHz, DMSO) δ 9.63 (1H, d, J = 8.5 Hz, NH), 9.48 (1H, s, NH), 9.08 (1H, s, NH), 8.74 (1H, s, H5′), 8.09 (1H, s, H4), 7.90 (2H, d, J = 8.9 Hz, Ph), 7.87 (1H, d, J = 8.4 Hz, H7), 7.71 (1H, d, J = 8.5 Hz, H6), 7.66 (2H, d, J = 8.8 Hz, Ph), 4.13–4.05 (1H, m, CH), 3.55 (2H, t, J = 7.2 Hz,CH_2), 3.42 (2H, t, J = 7.3 Hz, CH_2), 1.31 (6H, d, J = 6.4 Hz, $\underline{CH_3}C\underline{CH_3}$).^{13}C NMR (75 MHz, DMSO) δ 161.67, 156.58, 145.87, 141.03, 138.06, 135.41, 132.79, 129.87, 126.47, 124.30, 121.54, 120.91, 114.14, 45.15, 26.56, 22.66, 21.22. Anal. calcd. for $C_{21}H_{22}ClN_7$ x 2 HCl x 1.5 H_2O (Mr = 507.85): C 49.67, H 5.36, N 19.31; found: C 49.73, H 5.32, N 18.98%. HRMS: calcd. for $C_{21}H_{22}ClN_7$ $(M + H)^+$: 408.1703 found: 408.1687.

4.3. Cell culturing

Human cell lines A549 (lung carcinoma), HeLa (cervical carcinoma), SW620 (colorectal adenocarcinoma, metastatic) and CFPAC-1 (pancreatic cancer, derived from metastatic: liver) as well as WI38 (normal human lung fibroblasts) were cultured as monolayers and maintained in Dulbecco's modified Eagle medium (DMEM) supplemented with 10% fetal bovine serum (FBS), 2 mM L-glutamine, 100 U/ml penicillin and 100 μg/mL streptomycin in a humidified atmosphere with 5% CO_2 at 37 °C.

4.4. Proliferation assays

The panel cell lines were inoculated onto a series of standard 96-well microtiter plates on day 0, at 5000 cells per well according to the doubling times of specific cell line. Test agents were then added in five, 10-fold dilutions (0.01–100 μM) and incubated for further 72 h. Working dilutions were freshly prepared on the day of testing in the growth medium. The solvent (DMSO) was also tested for eventual inhibitory activity by adjusting its concentration to be the same as in the working concentrations (DMSO concentration never exceeded 0.1%). After 72 h of incubation, the cell growth rate was evaluated by performing the MTT assay: experimentally determined absorbance values were transformed into a cell percentage growth (PG) using the formulas proposed by NIH and described previously [73]. This method directly relies on control cells behaving normally at the day of assay because it compares the growth of treated cells with the growth of untreated cells in control wells on the same plate - the results are therefore a percentile difference from the calculated expected value. The IC_{50} and LC_{50} values for each compound were calculated from dose-response curves using linear regression analysis by fitting the mean test concentrations that give PG values above and below the reference value. If, however, all of the tested concentrations produce PGs exceeding the respective reference level of effect (*e.g.* PG value of 50) for a given cell line, the highest tested concentration is assigned as the default value (in the screening data report that default value is preceded by a ">" sign). Each test point was performed in quadruplicate in three individual experiments. The results were statistically analyzed (ANOVA, Tukey post-hoc test at $p < 0.05$). Finally, the effects of the tested substances were evaluated by plotting the mean percentage growth for each cell type in comparison to control on dose response graphs.

4.5. Western blot analysis

Cells were cultured in 6-well plates at seeding density of 200000 cells/well and subjected to treatment with selected compounds at their 2 × IC_{50} concentrations for 48 h. Cells were lysed in RIPA buffer containing 20 mM Tris-HCl (pH 7.5), 150 mM NaCl, 1 mM Na2 EDTA, 1 mM EGTA, 1% NP-40 and 1% sodium deoxycholate supplemented with protease inhibitor cocktail (Roche). Total proteins (50 μg) were resolved on 12% Tris-glycine polyacrylamide gels and transferred to PVDF membranes. Subsequently, membranes were blocked for 1 h at room temperature with 4% BSA in TBST [50 mmol/L Tris base, 150 mmol/L NaCl, 0.1% Tween 20 (pH 7.5)] and probed overnight at 4 °C with primary antibody against either PDE5 (Cell Signaling Technology), CDK9/cyclin T1 (Cell Signaling Technology), TGM2 ((Cell Signaling Technology), p-p53 (Ser15) (Abcam), p-SK1 (ECM Biosciences) and p-38 MAPK (Thr180/Tyr182). Membranes were washed with TBST and incubated with either goat anti-mouse (Santa Cruz Biotechnology) or goat anti-rabbit (Santa Cruz Biotechnology) horseradish peroxidase–conjugated secondary antibody at room temperature for 1 h. Individual proteins were visualized by the BM Chemiluminescence Western Blotting Substrate (POD) (Roche) using ImageQuant LAS 500 (GE Healthcare). Densitometry quantitation was determined using the Quantity One 1-D Analysis Software (Bio-Rad, USA).

4.6. Apoptosis detection

Detection and quantification of apoptosis and differentiation from necrosis at single cell level was carried out by Annexin-V-FITC Staining kit (Santa Cruz Biotech) according to the manufacturer's instructions. Briefly, cells were seeded into Lab-tek II Chamber Slide with 8 wells and treated with test compounds at their 2 × IC_{50} concentrations for 48 h. The cells were washed with Incubation buffer, and Annexin-V-FITC labelling solution was added. After incubation at room temperature for 15 min, chambers and silicon borders of the chamber slides were removed, the cells were fixed with 20% glycerol and analyzed by fluorescence microscopy.

4.7. In silico analysis

Predictions of plausible biological targets and pharmacological activities were made by web-service PASS (http://www.pharmaexpert.ru/passonline/index.php) which is based on the identification of substructure features typical for active molecules [52,74].

4.8. Computational methods

Available crystal structures of apo and co-crystalised p38-α kinase with various inhibitors were downloaded from protein data bank [75,76]. Due to the large number of available crystal structures (384 structures), downloaded ligands were clustered by Canvas similarity and clustering protocol [77,78] in order to obtain representative but chemicaly diverse set for further anaylsis. Representative ligands from the following DFG-in X-ray structure were used: 3LFA, 3MW1, 4EH3, 4FA2, 4KIN, 4ZTH, 4R3C, 3ZSH, 3C5U, 3FMK, 3HP5, 3BX5, 3ZYA, 1ZZ2. Representative ligands from the following DFG-out X-ray structures: 3HV6, 3HEC, 3LFE, 3IW8, 3P79, 3D83, 3K3J, 3P5K, 3P7A, 3P7b, 3P7C. Gly flip structures: 1OUK, 1OUY AND 1OVE for DFG-in conformation and 2YIW AND 4KIN for DFG-out conformation. IC_{50} inhibition values were collected from BindingDB [79]. Field based alignment of bio-active conformations of representative ligands was performed using Torch software from Cresset [80]. Conformational search was performed for compounds **10c** and **11f** while p38 inhibitors from Protein data bank were fixed in the bio-active conformation. Protein structure was used to define excluded volume and further restrict possible alignment options. The ligand docking studies were carried out using Glide docking protocol [81–83] within Schroedinger suite of software [84] with

Please cite this article in press as: A. Bistrović, et al., Design, synthesis and biological evaluation of novel benzimidazole amidines as potent multi-target inhibitors for the treatment of non-small cell lung cancer, European Journal of Medicinal Chemistry (2017), https://doi.org/10.1016/j.ejmech.2017.10.061

extra precision (XP). Docking was performed using both constrained interactions with hinge amino-acids Met109 and Gly110 as well as unconstrained docking. Binding poses were refined and binding energy was estimated using MM-GBSA [85–87] protocol and OPLS3 force-field with flexible residues distance being 5 Å.

Acknowledgements

We greatly appreciate the financial support of the Croatian Science Foundation (grant number IP–2013–11–5596), University of Rijeka research grants 13.11.1.1.11. and 13.11.2.1.12., and the access to equipment owned by the University of Rijeka within the project RISK “Development of University of Rijeka campus laboratory research infrastructure”, financed by the European Regional Development Fund.

Appendix A. Supplementary data

Supplementary data related to this article can be found at https://doi.org/10.1016/j.ejmech.2017.10.061.

References

[1] M. Reck, D.F. Heigener, T. Mok, J.C. Soria, K.F. Rabe, Management of non-small-cell lung cancer: recent developments, Lancet 382 (2013) 709–719, https://doi.org/10.1016/S0140-6736(13)61502-0.
[2] F.R. Khuri, Lung cancer and other pulmonary neoplasms, in: G. Lee, I.S. Andrew (Eds.), Goldman's Cecil Medicine, 25th ed, Saunders, New York, 2016, pp. 1303–1313.
[3] C.C. Tièche, R.W. Peng, P. Dorn, L. Froment, R.A. Schmid, T.M. Marti, Prolonged pemetrexed pretreatment augments persistence of cisplatin-induced DNA damage and eliminates resistant lung cancer stem-like cells associated with EMT, BMC Cancer 16 (2016) 125, https://doi.org/10.1186/s12885-016-2117-4.
[4] D.S. Ettinger, D.E. Wood, W. Akerley, L.A. Bazhenova, H. Borghaei, D.R. Camidge, R.T. Cheney, L.R. Chirieac, T.A. D'Amico, T.J. Dilling, M.C. Dobelbower, NCCN guidelines insights: non–small cell lung cancer, version 4.2016, J. Natl. Compr. Canc. Netw. 14 (2016) 255–264, https://doi.org/10.6004/jnccn.2016.0031.
[5] Y. Xiong, B.Y. Huang, J.Y. Yin, Pharmacogenomics of platinum-based chemotherapy in non-small cell lung cancer: focusing on DNA repair systems, Med. Oncol. 34 (2017) 48–64, https://doi.org/10.1007/s12032-017-0905-6.
[6] A. Jemal, R. Siegel, E. Ward, Y. Hao, J. Xu, M.J. Thun, Cancer statistics, 2009, CA Cancer J. Clin. 59 (2009) 225–249, https://doi.org/10.3322/caac.20006.
[7] E. Hafen, Kinases and phosphatases-a marriage is consummated, Science 280 (1998) 1212–1213, https://doi.org/10.1126/science.280.5367.1212.
[8] P. Cohen, The origins of protein phosphorylation, Nat. Cell Biol. 4 (2002) e127–e130, https://doi.org/10.1038/ncb0502-e127.
[9] J.A. Ubersax, J.E. Ferrell, Mechanisms of specificity in protein phosphorylation, Nat. Rev. Mol. Cell Biol. 8 (2007) 530–541, https://doi.org/10.1038/nrm2203.
[10] P. Blume-Jensen, T. Hunter, Oncogenic kinase signalling, Nature 411 (2001) 355–365, https://doi.org/10.1038/35077225.
[11] J. Brognard, T. Hunter, Protein kinase signaling networks in cancer, Curr. Opin. Genet. Dev. 21 (2011) 4–11, https://doi.org/10.1016/j.gde.2010.10.012.
[12] P. Singla, V. Luxami, K. Paul, Benzimidazole-biologically attractive scaffold for protein kinase inhibitors, RSC Adv. 4 (2014) 12422–12440.
[13] M. Munde, M. Lee, S. Neidle, R. Arafa, D.W. Boykin, Y. Liu, C. Bailly, W.D. Wilson, Induced fit conformational changes of a “reversed amidine” heterocycle: optimized interactions in a DNA minor groove complex, J. Am. Chem. Soc. 129 (2007) 5688–5698, https://doi.org/10.1021/ja069003n.
[14] W.D. Wilson, B. Nguyen, F.A. Tanious, A. Mathis, J.E. Hall, C.E. Stephens, D.W. Boykin, Dications that target the DNA minor groove: compound design and preparation, DNA interactions, cellular distribution and biological activity, Curr. Med. Chem. Anticancer Agents 5 (2005) 389–408, https://doi.org/10.2174/1568011054222319.
[15] P. Wu, T.E. Nielsen, M.H. Clausen, FDA-approved small-molecule kinase inhibitors, Trends Pharmacol. Sci. 36 (2015) 422–439, https://doi.org/10.1016/j.tips.2015.04.005.
[16] L. Garuti, M. Roberti, G. Bottegoni, Benzimidazole derivatives as kinase inhibitors, Curr. Med. Chem. 21 (2014) 2284–2298, https://doi.org/10.2174/0929867321666140217105714.
[17] W. Akhtar, M.F. Khan, G. Verma, G.M. Shaquiquzzaman, M.A. Rizvi, S.H. Mehdi, M. Akhter, M.M. Alam, Therapeutic evolution of benzimidazole derivatives in the last quinquennial period, Eur. J. Med. Chem. 126 (2017) 705–753.
[18] M.J. Akhtar, A.A. Siddiqui, A.A. Khan, Z. Ali, R.P. Dewangan, S. Pasha, M.S. Yar, Design, synthesis, docking and QSAR study of substituted benzimidazole linked oxadiazole as cytotoxic agents, EGFR and erbB2 receptor inhibitors, Eur. J. Med. Chem. 126 (2017) 853–869, https://doi.org/10.1016/j.ejmech.2016.12.014.
[19] K. Kubiński, M. Masłyk, A. Orzeszko, Benzimidazole inhibitors of protein kinase CK2 potently inhibit the activity of atypical protein kinase Rio1, Mol. Cell. Biochem. 426 (2017) 195–203, https://doi.org/10.1007/s11010-016-2892-x.
[20] E. Łukowska-Chojnacka, P. Wińska, M. Wielechowska, M. Poprzeczko, M. Bretner, Synthesis of novel polybrominated benzimidazole derivatives–potential CK2 inhibitors with anticancer and proapoptotic activity, Bioorg. Med. Chem. 24 (2016) 735–741, https://doi.org/10.1016/j.bmc.2015.12.041.
[21] M.A. Pagano, M. Andrzejewska, M. Ruzzene, S. Sarno, L. Cesaro, J. Bain, M. Elliott, F. Meggio, Z. Kazimierczuk, L.A. Pinna, Optimization of protein kinase CK2 inhibitors derived from 4,5,6,7-tetrabromobenzimidazole, J. Med. Chem. 47 (2004) 6239–6247, https://doi.org/10.1021/jm049854a.
[22] Y.A. Sonawane, M.A. Taylor, J.V. Napoleon, S. Rana, J.I. Contreras, A. Natarajan, Cyclin dependent Kinase 9 inhibitors for cancer therapy: miniperspective, J. Med. Chem. 59 (2016) 8667–8684, https://doi.org/10.1021/acs.jmedchem.6b00150.
[23] L. Carlino, G. Rastelli, Dual Kinase-bromodomain inhibitors in anticancer drug discovery: a structural and pharmacological perspective: miniperspective, J. Med. Chem. 59 (2016) 9305–9320, https://doi.org/10.1021/acs.jmedchem.6b00438.
[24] Z.A. Knight, H. Lin, K.M. Shokat, Targeting the cancer kinome through polypharmacology, Nat. Rev. Cancer 10 (2010) 130–137, https://doi.org/10.1038/nrc2787.
[25] N.P. Shah, J.M. Nicoll, B. Nagar, M.E. Gorre, R.L. Paquette, J. Kuriyan, C.L. Sawyers, Multiple BCR-ABL kinase domain mutations confer polyclonal resistance to the tyrosine kinase inhibitor imatinib (STI571) in chronic phase and blast crisis chronic myeloid leukemia. Cancer Cell 2 (202) 117–125. doi: 10.1016/S1535-6108(02)00096-X.
[26] J.A. Engelman, K. Zejnullahu, T. Mitsudomi, Y. Song, C. Hyland, J.O. Park, N. Lindeman, C.M. Gale, X. Zhao, J. Christensen, T. Kosaka, MET amplification leads to gefitinib resistance in lung cancer by activating ERBB3 signaling, Science 316 (2007) 1039–1043, https://doi.org/10.1126/science.1141478.
[27] M. Hasegawa, N. Nishigaki, Y. Washio, K. Kano, P.A. Harris, H. Sato, I. Mori, R.I. West, M. Shibahara, H. Toyoda, L. Wang, Discovery of novel benzimidazoles as potent inhibitors of TIE-2 and VEGFR-2 tyrosine kinase receptors, J. Med. Chem. 50 (2007) 4453–4470, https://doi.org/10.1021/jm0611051.
[28] J. Akhtar, A.A. Khan, Z. Ali, R. Haider, M.S. Yar, Structure-activity relationship (SAR) study and design strategies of nitrogen-containing heterocyclic moieties for their anticancer activities, Eur. J. Med. Chem. 125 (2017) 143–189, https://doi.org/10.1016/j.ejmech.2016.09.023.
[29] R. Determann, J. Dreher, K. Baumann, L. Preu, P.G. Jones, F. Totzke, C. Schächtele, M.H. Kubbutat, C. Kunick, 2-Anilino-4-(benzimidazol-2-yl) pyrimidines–A multikinase inhibitor scaffold with antiproliferative activity toward cancer cell lines, Eur. J. Med. Chem. 53 (2012) 254–263, https://doi.org/10.1016/j.ejmech.2012.04.007.
[30] B. Chu, F. Liu, L. Li, C. Ding, K. Chen, Q. Sun, Z. Shen, Y. Tan, C. Tan, Y. Jiang, A benzimidazole derivative exhibiting antitumor activity blocks EGFR and HER2 activity and upregulates DR5 in breast cancer cells, Cell Death Dis. 6 (2015) e1686, https://doi.org/10.1038/cddis.2015.25.
[31] Y. Li, C. Tan, C. Gao, C. Zhang, X. Luan, X. Chen, H. Liu, Y. Chen, Y. Jiang, Discovery of benzimidazole derivatives as novel multi-target EGFR, VEGFR-2 and PDGFR kinase inhibitors, Bioorg. Med. Chem. 19 (2011) 4529–4535, https://doi.org/10.1016/j.bmc.2011.06.022.
[32] B.B. Hasinoff, X. Wu, J.L. Nitiss, R. Kanagasabai, J.C. Yalowich, The anticancer multi-kinase inhibitor dovitinib also targets topoisomerase I and topoisomerase II, Biochem. Pharmacol 84 (2012) 1617–1626, https://doi.org/10.1016/j.bcp.2012.09.023.
[33] T. Gregorić, M. Sedić, P. Grbčić, A.T. Paravić, S.K. Pavelić, M. Cetina, R. Vianello, S. Raić-Malić, Novel pyrimidine-2,4-dione–1,2,3-triazole and furo [2,3-*d*] pyrimidine-2-one–1,2,3-triazole hybrids as potential anti-cancer agents: synthesis, computational and X-ray analysis and biological evaluation, Eur. J. Med. Chem. 125 (2017) 1247–1267, https://doi.org/10.1016/j.ejmech.2016.11.028.
[34] M. Liu, Y. Hou, W. Yin, S. Zhou, P. Qian, Z. Guo, L. Xu, Y. Zhao, Discovery of a novel 6,7-disubstituted-4-(2-fluorophenoxy) quinolines bearing 1,2,3-triazole-4-carboxamide moiety as potent c-Met kinase inhibitors, Eur. J. Med. Chem. 119 (2016) 96–108, https://doi.org/10.1016/j.ejmech.2016.04.035.
[35] M. Vojtičková, J. Dobiaš, G. Hanquet, G. Addová, R. Cetin-Atalay, D.C. Yildirim, A. Boháč, Ynamide Click chemistry in development of triazole VEGFR2 TK modulators, Eur. J. Med. Chem. 103 (2015) 105–122, https://doi.org/10.1016/j.ejmech.2015.08.012.
[36] Y. Kommagalla, S. Cornea, R. Riehle, V. Torchilin, A. Degterev, C.V. Ramana, Optimization of the anti-cancer activity of the phosphatidylinositol-3 kinase pathway inhibitor PITENIN-1: switching thiourea with 1,2,3-triazole, MedChemComm 5 (2014) 1359–1363, https://doi.org/10.1039/C4MD00109E.
[37] A. Lebeau, C. Abrioux, D. Benimelis, Z. Benfodda, P. Meffre, Synthesis of 1,4-disubstituted 1,2,3-triazole derivatives using click chemistry and their Src Kinase activities, Med. Chem. 13 (2014) 40–48, https://doi.org/10.2174/1573406412666160404125718.
[38] A. Kumar, I. Ahmad, B.S. Chhikara, R. Tiwari, D. Mandal, K. Parang, Synthesis of 3-phenylpyrazolopyrimidine-1,2,3-triazole conjugates and evaluation of their Src kinase inhibitory and anticancer activities, Bioorg. Med. Chem. Lett. 21 (2011) 1342–1346, https://doi.org/10.1016/j.bmcl.2011.01.047.
[39] D. Kumar, V.B. Reddy, A. Kumar, D. Mandal, R. Tiwari, K. Parang, Click

chemistry inspired one-pot synthesis of 1,4-disubstituted 1,2,3-triazoles and their Src kinase inhibitory activity, Bioorg. Med. Chem. Lett. 21 (2011) 449–452, https://doi.org/10.1016/j.bmcl.2010.10.121.
[40] Z.Y. Cheng, W.J. Li, F. He, J.M. Zhou, X.F. Zhu, Synthesis and biological evaluation of 4-aryl-5-cyano-2H-1,2,3-triazoles as inhibitor of HER2 tyrosine kinase, Bioorg. Med. Chem. 15 (2007), https://doi.org/10.1016/j.bmc.2006.09.041, 533–1538.
[41] H.C. Kolb, K.B. Sharpless, The growing impact of click chemistry on drug discovery, Drug Discov. Today 8 (2003) 1128–1137, https://doi.org/10.1016/S1359-6446(03)02933-7.
[42] M. Song, H. Hwang, C.Y. Im, S.Y. Kim, Recent progress in the development of transglutaminase 2 (TGase2) inhibitors, J. Med. Chem. 60 (2017) 554–557, https://doi.org/10.1021/acs.jmedchem.6b01036.
[43] C. Pardin, J.N. Pelletier, W.D. Lubell, J.W. Keillor, Cinnamoyl inhibitors of tissue transglutaminase, J. Org. Chem. 73 (2008) 5766–5775, https://doi.org/10.1021/jo8004843.
[44] T.G. Kraljević, A. Harej, M. Sedić, S.K. Pavelić, V. Stepanić, D. Drenjančević, J. Talapko, S. Raić-Malić, Synthesis, in vitro anticancer and antibacterial activities and in silico studies of new 4-substituted 1, 2, 3-triazole–coumarin hybrids, Eur. J. Med. Chem. 124 (2016) 794–808, https://doi.org/10.1016/j.ejmech.2016.08.062.
[45] I. Stolić, K. Mišković, I. Piantanida, M.B. Lončar, Lj Glavaš-Obrovac, M. Bajić, Synthesis, DNA/RNA affinity and antitumour activity of new aromatic diamidines linked by 3,4-ethylenedioxythiophene, Eur. J. Med. Chem. 46 (2011) 743–755, https://doi.org/10.1016/j.ejmech.2010.12.010.
[46] R.N. Baig, R.S. Varma, Alternative energy input: mechanochemical, microwave and ultrasound-assisted organic synthesis, Chem. Soc. Rev. 41 (2012) 1559–1584, https://doi.org/10.1039/C1CS15204A.
[47] C.O. Kappe, E. Van der Eycken, Click chemistry under non-classical reaction conditions, Chem. Soc. Rev. 39 (2010) 1280–1290, https://doi.org/10.1039/B901973C.
[48] G. Cravotto, E.C. Gaudino, P. Cintas, On the mechanochemical activation by ultrasound, Chem. Soc. Rev. 42 (2013) 7521–7534, https://doi.org/10.1039/C2CS35456J.
[49] K.A. Ohemeng, V.N. Nguyen, Ortho Pharmaceutical Corporation, 2-substituted Phenyl-benzimidazole Antibacterial Agents. U.S. Patent Application 08/924,558, 1999. WO1999011627A1.
[50] M. Hranjec, K. Starčević, B. Zamola, S. Mutak, M. Derek, G. Karminski-Zamola, New amidino-benzimidazolyl derivatives of tylosin and desmycosin, J. Antibiot. 55 (2002) 308–314, https://doi.org/10.7164/antibiotics.55.308.
[51] N.R. Glover, G.C. MacDonald, J. Entwistle, J. Cizeau, D.G. Bosc, F.C. Chahal, Viventia Bio Inc, Tumor Specific Antibody. U.S. Patent Application 14/604,047, 2015. WO2015/092713.
[52] D.A. Filimonov, V.V. Poroikov, in: A. Varnek, A. Tropsha (Eds.), Chemoinformatics Approaches to Virtual Screening, RSC Publishing, Cambridge, UK, 2008, pp. 182–216.
[53] C.M. Whitehead, K.A. Earle, J. Fetter, S. Xu, T. Hartman, D.C. Chan, T.L. Zhao, G. Piazza, A.J. Klein-Szanto, R. Pamukcu, H. Alila, Exisulind-induced apoptosis in a non-small cell lung cancer orthotopic lung tumor model augments docetaxel treatment and contributes to increased survival, Mol. Cancer Ther. 2 (2003) 479–488.
[54] T. Yin, M.J. Lallena, E.L. Kreklau, K.R. Fales, S. Carballares, R. Torrres, G.N. Wishart, R.T. Ajamie, D.M. Cronier, P.W. Iversen, T.I. Meier, A novel CDK9 inhibitor shows potent antitumor efficacy in preclinical hematologic tumor models, Mol. Cancer Ther. 13 (2014) 1442–1456, https://doi.org/10.1158/1535-7163.MCT-13-0849.
[55] A. Bagashev, S. Fan, R. Mukerjee, P. Paolo Claudio, T. Chabrashvili, R.P. Leng, S. Benchimol, B.E. Sawaya, Cdk9 phosphorylates Pirh2 protein and prevents degradation of p53 protein, Cell Cycle 12 (2013) 1569–1577, https://doi.org/10.4161/cc.24733.
[56] S. Mishra, L.J. Murphy, The p53 oncoprotein is a substrate for tissue transglutaminase kinase activity, Biochem. Bioph. Res. Co. 339 (2006) 726–730, https://doi.org/10.1016/j.bbrc.2005.11.071.
[57] C.M. Choi, S.J. Jang, S.Y. Park, Y.B. Choi, J.H. Jeong, D.S. Kim, H.K. Kim, K.S. Park, B.H. Nam, H.R. Kim, S.Y. Kim, Transglutaminase 2 as an independent prognostic marker for survival of patients with non-adenocarcinoma subtype of non-small cell lung cancer, Mol. Cancer 10 (2011) 119, https://doi.org/10.1186/1476-4598-10-119.
[58] L. Song, H. Xiong, J. Li, W. Liao, L. Wang, J. Wu, M. Li, Sphingosine Kinase-1 enhances resistance to apoptosis through activation of PI3K/Akt/NF-κb pathway in human non–small cell lung cancer, Clin. Cancer Res. 17 (2011) 1839–1849, https://doi.org/10.1158/1078-0432.CCR-10-0720.
[59] L. Zhu, Z. Wang, Y. Lin, Z. Chen, H. Liu, Y. Chen, N. Wang, X. Song, Sphingosine kinase 1 enhances the invasion and migration of non-small cell lung cancer cells via the AKT pathway, Oncol. Rep. 33 (2015) 1257–1263.
[60] V. Schenten, C. Melchior, N. Steinckwich, E.J. Tschirhart, S. Bréchard, Sphingosine kinases regulate NOX2 activity via p38 MAPK-dependent translocation of S100A8/A9, J. Leukoc. Biol. 89 (2011) 587–596, https://doi.org/10.1189/jlb.0510304.
[61] M.M. Adada, K.A. Orr-Gandy, A.J. Snider, D. Canals, Y.A. Hannun, L.M. Obeid, C.J. Clarke, Sphingosine kinase 1 regulates tumor necrosis factor-mediated RANTES induction through p38 mitogen-activated protein kinase but independently of nuclear factor κB activation, J. Biol. Chem. 288 (2013) 27667–27679, https://doi.org/10.1074/jbc.M113.489443.
[62] Q.B. She, N. Chen, Z. Dong, ERKs and p38 kinase phosphorylate p53 protein at serine 15 in response to UV radiation, J. Biol. Chem. 275 (2000) 20444–20449, https://doi.org/10.1074/jbc.M001020200.
[63] R. Sanchez-Prieto, J.M. Rojas, Y. Taya, J.S. Gutkind, A role for the p38 mitogen-activated protein kinase pathway in the transcriptional activation of p53 on genotoxic stress by chemotherapeutic agents, Cancer Res. 60 (2000) 2464–2472.
[64] A. Patnaik, P. Haluska, A.W. Tolcher, C. Erlichman, K.P. Papadopoulos, J.L. Lensing, M. Beeram, J.R. Molina, D. Rasco, R.R. Arcos, C.S. Kelly, A first-in-human phase i study of the oral p38 MAPK inhibitor, ralimetinib (LY2228820 Dimesylate), in patients with advanced cancer, Clin. Cancer Res. 22 (2016) 1095–1102, https://doi.org/10.1158/1078-0432.CCR-15-1718.
[65] R.S.K. Vijayan, P. He, V. Modi, K.C. Duong-Ly, H. Ma, J.R. Peterson, R.L. Dunbrack Jr., R.M. Levy, Conformational analysis of the DFG-out kinase motif and biochemical profiling of structurally validated type II inhibitors, J. Med. Chem. 58 (2015) 466–479, https://doi.org/10.1021/jm501603h.
[66] C.E. Fitzgerald, S.B. Patel, J.W. Becker, P.M. Cameron, D. Zaller, V.B. Pikounis, S.J. O'Keefe, G. Scapin, Structural basis for p38α MAP kinase quinazolinone and pyridol-pyrimidine inhibitor specificity, Nat. Struct. Mol. Biol. 10 (2003) 764–769, https://doi.org/10.1038/nsb949.
[67] D.S. Millan, M.E. Bunnage, J.L. Burrows, K.J. Butcher, P.G. Dodd, T.J. Evans, D.A. Fairman, S.J. Hughes, I.C. Kilty, A. Lemaitre, R.A. Lewthwaite, Design and synthesis of inhaled p38 inhibitors for the treatment of chronic obstructive pulmonary disease, J. Med. Chem. 54 (2011) 7797–7814, https://doi.org/10.1021/jm200677b.
[68] P.A. Greenidge, C. Kramer, J.C. Mozziconacci, R.M. Wolf, MM/GBSA binding energy prediction on the PDBbind data set: successes, failures, and directions for further improvement, J. Chem. Inf. Model 53 (2012) 201–209, https://doi.org/10.1021/ci300425v.
[69] N.T. Chandrika, S.K. Shrestha, H.X. Ngo, S. Garneau-Tsodikova, Synthesis and investigation of novel benzimidazole derivatives as antifungal agents, Bioorg. Med. Chem. 24 (2016) 3680–3686, https://doi.org/10.1016/j.bmc.2016.06.010.
[70] R. Kumar, J. Arora, A.K. Prasad, N. Islam, A.K. Verma, Synthesis and antimicrobial activity of pyrimidine chalcones, Med. Chem. Res. 22 (2013) 5624–5631, https://doi.org/10.1007/s00044-013-0555-y.
[71] P.V. Chavan, K.S. Pandit, U.V. Desai, M.A. Kulkarni, P.P. Wadgaonkar, Cellulose supported cuprous iodide nanoparticles (Cell-CuI NPs): a new heterogeneous and recyclable catalyst for the one pot synthesis of 1,4-disubstituted–1,2,3-triazoles in water, RSC Adv. 4 (2014) 42137–42146, https://doi.org/10.1039/C4RA05080K.
[72] N. Boechat, V.F. Ferreira, S.B. Ferreira, M.D.L.G. Ferreira, F.D.C. da Silva, M.M. Bastos, M.D.S. Costa, M.C.S. Lourenco, A.C. Pinto, A.U. Krettli, A.C. Aguiar, Novel 1, 2, 3-triazole derivatives for use against Mycobacterium tuberculosis H37Rv (ATCC 27294) strain, J. Med. Chem. 54 (2011) 5988–5999, https://doi.org/10.1021/jm2003624.
[73] T. Gazivoda, S. Raić-Malić, V. Krištafor, D. Makuc, J. Plavec, S. Kraljević-Pavelić, K. Pavelić, L. Naesens, G. Andrei, R. Snoeck, J. Balzarini, M. Mintas, Synthesis, cytostatic and anti-HIV evaluations of the new unsaturated acyclic C-5 pyrimidine nucleoside analogues, Bioorg. Med. Chem. 16 (2008) 5624–5634, https://doi.org/10.1016/j.bmc.2008.03.074.
[74] K.R. Patil, P. Mohapatra, H.M. Patel, S.N. Goyal, S. Ojha, C.N. Kundu, C.R. Patil, Pentacyclic triterpenoids inhibit IKKβ mediated activation of NF-κB pathway: in silico and in vitro evidences, PLoS One 10 (2015), e0125709, https://doi.org/10.1371/journal.pone.0125709.
[75] RSC PDB, http://www.rcsb.org/pdb/, 2017 (accessed 31.03.17).
[76] H.M. Berman, J. Westbrook, Z. Feng, G. Gilliland, T.N. Bhat, H. Weissig, I.N. Shindyalov, P.E. Bourne, The protein data bank, Nucleic Acids Res. 28 (2000) 235–242, https://doi.org/10.1093/nar/28.1.235.
[77] J. Duan, S.L. Dixon, J.F. Lowrie, W. Sherman, Analysis and comparison of 2D fingerprints: insights into database screening performance using eight fingerprint methods, J. Mol. Graph. Model 29 (2010) 157–170, https://doi.org/10.1016/j.jmgm.2010.05.008.
[78] M. Sastry, J.F. Lowrie, S.L. Dixon, W. Sherman, Large-scale systematic analysis of 2D fingerprint methods and parameters to improve virtual screening enrichments, J. Chem. Inf. Model 50 (2010) 771–784, https://doi.org/10.1021/ci100062n.
[79] X. Chen, Y. Lin, M.K. Gilson, The binding database: overview and user's guide, Biopolymers 61 (2001) 127–141.
[80] Torch, Version 10.4.1., Cresset, Litlington, Cambridgeshire, UK, http://www.cresset-group.com/torch/.
[81] R.A. Friesner, R.B. Murphy, M.P. Repasky, L.L. Frye, J.R. Greenwood, T.A. Halgren, P.C. Sanschagrin, D.T. Mainz, Extra precision glide: docking and scoring incorporating a model of hydrophobic enclosure for protein–ligand complexes, J. Med. Chem. 49 (2006) 6177–6196, https://doi.org/10.1021/jm051256o.
[82] T.A. Halgren, R.B. Murphy, R.A. Friesner, H.S. Beard, L.L. Frye, W.T. Pollard, J.L. Banks, Glide: a new approach for rapid, accurate docking and scoring. 2. Enrichment factors in database screening, J. Med. Chem. 47 (2004) 1750–1759, https://doi.org/10.1021/jm030644s.
[83] R.A. Friesner, J.L. Banks, R.B. Murphy, T.A. Halgren, J.J. Klicic, D.T. Mainz, M.P. Repasky, E.H. Knoll, M. Shelley, J.K. Perry, D.E. Shaw, Glide: a new approach for rapid, accurate docking and scoring. 1. Method and assessment of docking accuracy, J. Med. Chem. 47 (2004) 1739–1749, https://doi.org/10.1021/jm0306430.
[84] Schrödinger Release 2017-1, MacroModel, Schrödinger, LLC, New York, NY,

Please cite this article in press as: A. Bistrović, et al., Design, synthesis and biological evaluation of novel benzimidazole amidines as potent multi-target inhibitors for the treatment of non-small cell lung cancer, European Journal of Medicinal Chemistry (2017), https://doi.org/10.1016/j.ejmech.2017.10.061

2017.
[85] J. Li, R. Abel, K. Zhu, Y. Cao, S. Zhao, R.A. Friesner, The VSGB 2.0 model: a next generation energy model for high resolution protein structure modeling, Proteins 79 (2011) 2794–2812, https://doi.org/10.1002/prot.23106.
[86] W.L. Jorgensen, D.S. Maxwell, J. Tirado-Rives, Development and testing of the OPLS all-atom force field on conformational energetics and properties of organic liquids, J. Am. Chem. Soc. 118 (1996) 11225–11236, https://doi.org/10.1021/ja9621760.
[87] D. Shivakumar, J. Williams, Y. Wu, W. Damm, J. Shelley, W. Sherman, Prediction of absolute solvation free energies using molecular dynamics free energy perturbation and the OPLS force field, J. Chem. Theory Comput. 6 (2010) 1509–1519, https://doi.org/10.1021/ct900587b.

Please cite this article in press as: A. Bistrović, et al., Design, synthesis and biological evaluation of novel benzimidazole amidines as potent multi-target inhibitors for the treatment of non-small cell lung cancer, European Journal of Medicinal Chemistry (2017), https://doi.org/10.1016/j.ejmech.2017.10.061